Inorg. Chem. **2006**, *45*, 1445–1462

Asymmetric Transformation of a Double-Stranded, Dicopper(I) Helicate Containing Achiral Bis(bidentate) Schiff Bases

Nicolle C. Habermehl,[†] Patricia M. Angus,[‡] Nathan L. Kilah,[†] Lasse Norén,[†] A. David Rae,[†] Anthony C. Willis,[†] and S. Bruce Wild*[,†]

Research School of Chemistry, Institute of Advanced Studies, Australian National University, Canberra, ACT 0200, Australia, and Department of Chemistry, Faculty of Science, Australian National University, Canberra, ACT 0200, Australia

Received August 29, 2005

Reactions of the bis(bidentate) Schiff-bases *N*,*N*′-bis(6-alkyl-2-pyridylmethylene)ethane-1,2-diamine (where alkyl = H, Me, ^{i}Pr) (L) with tetrakis(acetonitrile)copper(I) hexafluorophosphate and silver(I) hexafluorophosphate afforded, respectively, the double-stranded, dinuclear metal helicates [*T*-4-(*R**,*R**)]-(±)-$[M_2L_2](PF_6)_2$ (M = Cu, Ag). The helicates were characterized by ^{1}H and ^{13}C NMR spectroscopy, conductivity, microanalysis, and single-crystal X-ray structure determinations on selected compounds. Intermolecular ligand exchange and intramolecular inversion rates for the complexes were investigated by ^{1}H NMR spectroscopy. Reversible intermolecular ligand exchange between two differently substituted helicates followed first-order kinetics. The rate constants (k) and corresponding half-lives ($t_{1/2}$) for ligand exchange for the dicopper(I) helicates were $k = (1.6–1.8) \times 10^{-6}$ s^{-1} ($t_{1/2}$ = 110–120 h) in acetone-d_6, $k = 4.9 \times 10^{-6}$ s^{-1} ($t_{1/2}$ = 40 h) in dichloromethane-d_2, and $k > 2 \times 10^{-3}$ s^{-1} ($t_{1/2}$ < 5 min) in acetonitrile-d_3. Ligand exchange for the disilver(I) helicates occurred with $k > 2 \times 10^{-3}$ s^{-1} ($t_{1/2}$ < 5 min). Racemization of the dicopper(I) helicate by an intramolecular mechanism was investigated by determination of the coalescence temperature for the diastereotopic isopropyl-*Me* groups in the appropriate complex, and $\Delta G^{\ddagger} \gg 76$ kJ mol^{-1} was calculated for the process in acetone-d_6, nitromethane-d_3, and dichloromethane-d_2 with $\Delta G^{\ddagger} = 75$ kJ mol^{-1} in acetonitrile-d_3. Complete anion exchange of the hexafluorophosphate salt of a dicopper(I) helicate with the enantiomerically pure Δ-(−)-tris(catecholato)arsenate(V) ($[As(cat)_3]^-$) in the presence of Dabco gave the two diastereomers (*R*,*R*)-$[Cu_2L_2]$-$\{\Delta$-(−)-$[As(cat)_3]\}_2$ and (*S*,*S*)-$[Cu_2L_2]\{\Delta$-(−)-$[As(cat)_3]\}_2$ in up to 54% diastereomeric excess, as determined by ^{1}H NMR spectroscopy. The diastereomerically and enantiomerically pure salt (*R*,*R*)-$[Cu_2L_2]\{\Delta$-(−)-$[As(cat)_3]\}_2$ crystallized from the solution in a typical second-order asymmetric transformation. The asymmetric transformation of the dicopper(I) helicate is the first synthesis of a diastereomerically and enantiomerically pure dicopper(I) helicate containing achiral ligands.

Introduction

Helicates are a type of chiral coordination compound and are often included in the broad area of supramolecular chemistry,[1] with particular interest being ascribed to their "self-assembling" properties.[2] Despite chirality being inherent in these coordination compounds, few resolutions of helicates have been reported. The spontaneous resolution of a neutral, triple-stranded diiron(III) helicate[3] and the "partial spontaneous resolution" of a triple-stranded trinickel(II) helicate have been reported.[4] (The spontaneous resolution of a double-stranded dicopper(I) helicate was incorrectly claimed[5]—the compound crystallizes in the space group *Cc* and so the cation cannot be present as a single enantiomer.) The

* To whom correspondence should be addressed. E-mail: sbw@rsc.anu.edu.au.
† Institute of Advanced Studies.
‡ Faculty of Science.

(1) Lehn, J.-M. *Supramolecular Chemistry*; VCH: Weinheim, Germany, 1995. Piguet, C.; Bernardinelli, G.; Hopfgartner, G. *Chem. Rev.* **1997**, *97*, 2005. Albrecht, M. *Chem. Rev.* **2001**, *101*, 3457. Constable, E. C. *Prog. Inorg. Chem.* **1994**, *42*, 67. Constable, E. C. *Metals and Ligand Reactivity*; VCH: Weinheim, Germany, 1996; pp. 212−220. Williams, A. *Chem.*—Eur. J. **1997**, *3*, 15. Williams, A. F. *Chimia* **2000**, *54*, 585. Provent, C.; Williams, A. F. In *Transition Metals in Supramolecular Chemistry*; Sauvage, J.-P., Ed.; John Wiley & Sons: Chichester, U.K., 1999; Vol. 5, Chapter 4.
(2) Swiegers, G. F.; Malefestse, T. J. *Chem. Rev.* **2000**, *100*, 3483. Machado, V. G.; Baxter, P. N. W.; Lehn, J.-M. *J. Braz. Chem. Soc.* **2001**, *12*, 431.
(3) Scarrow, R. C.; White, D. L.; Raymond, K. N. *J. Am. Chem. Soc.* **1985**, *107*, 6540.

10.1021/ic051478c CCC: $33.50
Published on Web 01/27/2006

chromatographic resolution of double- and triple-stranded di- and trinuclear metal helicates has been accomplished using aqueous sodium antimonyl (+)-tartrate or aqueous sodium (−)-bis(*p*-tolyl)tartrate as the eluant on Sephadex-SP C-25 ion exchange columns[6] and by use of Whatman 3MM CHR chromatography paper (cellulose) as the chiral stationary phase (elution with aqueous sodium chloride).[7] Diastereomerically enriched salts of a diiron(II) helicate have been generated with use of the enantiomerically pure anion Δ-tris(tetrachlorocatecholato)phosphate, with >96% diastereomeric excess (de) being observed for the two diastereomers, as determined by ^{1}H NMR spectroscopy.[8] The selective crystallization of one diastereomer of a triple-stranded digallate(III) helicate in the presence of (*S*)-*N*-methylnicotinium iodide has also been reported.[9]

VT-NMR spectroscopy has been used to determine energy barriers for inversion of helicate configuration by coalescence of diastereotopic isopropyl-*Me* resonances[10] or by coalescence of diastereotopic methylene-*H* resonances.[11−15] Racemization by an intramolecular mechanism was found to occur for a triple-stranded digallium(III) helicate (sequential Bailar twists of the metal centers)[10] and for a triple-stranded dititanium(IV) helicate.[11] Racemization of a double-stranded (nonchelating) dipalladium(II) helicate was suggested to occur by intermolecular ligand exchange.[16] The rate of racemization has been measured by CD spectroscopy for an enantiomerically pure, triple-stranded dicobalt(II) helicate;[17] the mechanism of racemization of the complex by ligand exchange was followed by ES mass spectrometry.[18] The barriers to inversion of double-stranded (nonchelating) dicopper(I) helicates have been determined.[12] In dimethylformamide-d_7, barriers ranging from $\Delta G^{\ddagger}_{298} = 50.6$ kJ mol^{-1} ($T_c = 274$ K) to 73.4 kJ mol^{-1} ($T_c = 359$ K) were found. Stability constants for the complexes were determined to be in the range log β 12.8−16.0 in dimethylformamide. Correlation of the observed stability constants with the free energy barriers to racemization supported a dissociative mechanism of racemization via the species $[CuL_2]^+$. The barrier to racemization of a double-stranded dicopper(I) helicate containing bis(bipyridyl) ligands was determined from VT-NMR spectroscopy to be $\Delta G^{\ddagger} > 88$ kJ mol^{-1} in nitromethane-d_3 (estimated $T_c \geq 433$ K).[13] Similarly, a double-stranded trisilver(I) helicate gave $\Delta G^{\ddagger} = 69.5$ kJ mol^{-1} in dimethyl sulfoxide-d_6 ($T_c = 335$ K), but the NMR spectrum of the analogous copper(I) helicate was unchanged on heating to 90 °C.[14] A double-stranded dicopper(I) helicate containing an unsymmetrical ligand was determined to have a barrier to inversion of $\Delta G^{\ddagger}_{298} = 69.5$ kJ mol^{-1} (acetonitrile-d_3), but no details, such as the occurrence of head-to-head−head-to-tail isomerism, were given.[15]

The attempted resolutions and kinetics of inversion of tetrahedral bis(bidentate)metal complexes have been reviewed.[19] The labilities of such complexes generally preclude isolation of the enantiomerically pure compounds, even though the separation of diastereomers is possible. Chiral monocopper(I) complexes of the type $[Cu(AB)_2]^+$ readily undergo intermolecular ligand exchange and intramolecular inversion of the metal stereocenter. Rates of intermolecular ligand exchange and intramolecular inversion have been measured for bis(bidentate)copper(I) complexes containing achiral[20] and chiral diimine ligands.[21] The rates of racemization at copper were lowered by the introduction of bulky substituents ortho to the donor atoms of the ligand. The configurational stabilities of monocopper(I) complexes containing achiral ligands, but associated with a chiral anion, have recently been reported.[22] The coalescence temperatures relating to the inversion of a macrocyclic, dicopper(I) complex containing an N_4S_4 donor system have been determined.[23]

Mononuclear copper(I) complexes have been synthesized diastereoselectively or in diastereomeric excess by use of chiral ligands.[24] The spontaneous resolution of a copper(I) complex containing a macrocyclic N_2S_2-donor ligand with a twisted biphenyl bridge has been achieved.[25] The first-order asymmetric transformations of copper(I) complexes

(4) Krämer, R.; Lehn, J.-M.; De Cian, A.; Fischer, J. *Angew. Chem., Int. Ed. Engl.* **1993**, *32*, 703.
(5) Baxter, P. N. W.; Lehn, J.-M.; Rissanen, K. *Chem. Commun.* **1997**, 1323.
(6) Hasenknopf, B.; Lehn, J.-M. *Helv. Chim. Acta* **1996**, *79*, 1643. Charbonniere, L. J.; Bernardinelli, G.; Piguet, C.; Sargeson, A. M.; Williams, A. F. *Chem. Commun.* **1994**, 1419. Rapenne, G.; Patterson, B. T.; Sauvage, J.-P.; Keene, F. R. *J. Chem. Soc., Chem. Commun.* **1999**, 1853.
(7) Hannon, M. J.; Meistermann, I.; Isaac, C. J.; Blomme, C.; Aldrich-Wright, J. R.; Rodger, A. *Chem. Commun.* **2001**, 1078.
(8) Jodry, J. J.; Lacour, J. *Chem.*—Eur. J. **2000**, *6*, 4297.
(9) Yeh, R. M.; Ziegler, M.; Johnson, D. W.; Terpin, A. J.; Raymond, K. N. *Inorg. Chem.* **2001**, *40*, 2216.
(10) Meyer, M.; Kersting, B.; Powers, R. E.; Raymond, K. N. *Inorg. Chem.* **1997**, *36*, 5179. Kersting, B.; Meyer, M.; Powers, R. E.; Raymond, K. N. *J. Am. Chem. Soc.* **1996**, *118*, 7221.
(11) Albrecht, M.; Schneider, M.; Röttele, H. *Chem. Ber./Recueil* **1997**, *130*, 615. Albrecht, M.; Schneider, M. *J Chem. Soc., Chem. Commun.* **1998**, 137.
(12) Carina, R. F.; Williams, A. F.; Piguet, C. *Helv. Chim. Acta* **1998**, *81*, 548.
(13) Lehn, J.-M.; Rigault, A.; Siegel, J.; Harrowfield, J.; Chevrier, B.; Moras, D. *Proc. Natl. Acad. Sci. U.S.A.* **1987**, *84*, 2565.
(14) Greenwald, M.; Wessely, D.; Goldberg, I.; Cohen, Y. *New J. Chem.* **1999**, *23*, 337.
(15) Mathieu, J.; Marsura, A.; Bouhmaida, N.; Ghermani, N. *Eur. J. Inorg. Chem.* **2002**, 2433.
(16) Mazet, C.; Gade, L. H. *Chem.*—Eur. J. **2002**, *8*, 4308.
(17) Charbonnière, L. J.; Gilet, M.-F.; Bernauer, K.; Williams, A. F. *Chem. Commun.* **1996**, 39.
(18) Charbonnière, L. J.; Williams, A. F.; Frey, U.; Merbach, A. E.; Kamalaprija, P.; Schaad, O. *J. Am. Chem. Soc.* **1997**, *119*, 2488.
(19) Basolo, F.; Pearson, R. G. *Mechanisms of Inorganic Reactions*; John Wiley & Sons: New York, 1958; pp 283−285. Holm, R. H.; O'Connor, M. J. *Prog. Inorg. Chem.* **1971**, *14*, 241. Minkin, V. I.; Nivorozhkin, L. E.; Korobov, M. S. *Russ. Chem. Rev.* **1994**, *63*, 289.
(20) Frei, U. M.; Geier, G. *Inorg. Chem.* **1992**, *31*, 187. Frei, U. M.; Geier, G. *Inorg. Chem.* **1992**, *31*, 3132. Riesgo, E.; Hu, Y.-Z.; Bouvier, F.; Thummel, R. P. *Inorg. Chem.* **2001**, *40*, 2541.
(21) van Stein, G. C.; van Koten, G.; de Bok, B.; Taylor, L. C.; Vrieze, K.; Brevard, C. *Inorg. Chim. Acta* **1984**, *89*, 29. Pianet, I.; Vincent, J.-M. *Inorg. Chem.* **2004**, *43*, 2947.
(22) Desvergnes-Breuil, V.; Hebbe, V.; Dietrich-Buchecker, C.; Sauvage, J.-P.; Lacour, J. *Inorg. Chem.* **2003**, *42*, 255.
(23) Comba, P.; Fath, A.; Hambley, T. W.; Kühner, A.; Richens, D. T.; Vielfort, A. *Inorg. Chem.* **1998**, *37*, 4389.
(24) Riesgo, E. C.; Credi, A.; De Cola, L.; Thummel, R. P. *Inorg. Chem.* **1998**, *37*, 2145. Vincent, J.-M.; Philouze, C.; Pianet, I.; Verlhac, J.-B. *Chem.*—Eur. J. **2000**, *6*, 3595. Regnouf-de-Vains, J.-B.; Lamartine, R.; Fenet, B. *Helv. Chim. Acta* **1998**, *81*, 661. Nabeshima, T.; Hashiguchi, A.; Saiki, T.; Akine, S. *Angew. Chem., Int. Ed.* **2002**, *41*, 481.
(25) Flanagan, S.; Dong, J.; Haller, K.; Wang, S.; Scheidt, W. R.; Scott, R. A.; Webb, T. R.; Stanbury, D. M.; Wilson, L. J. *J. Am. Chem. Soc.* **1997**, *119*, 8857.

Scheme 1

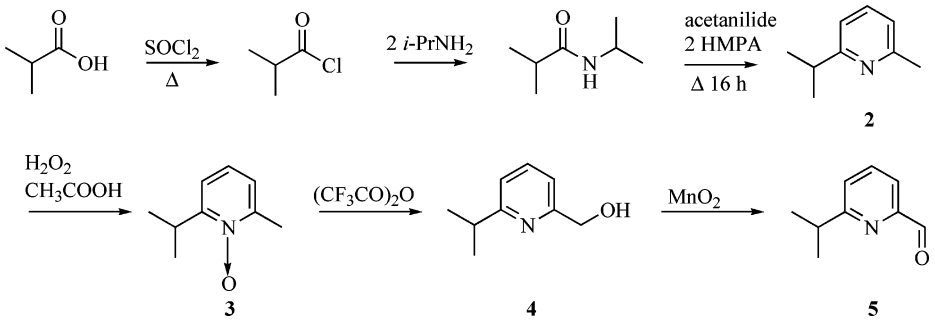

have been accomplished by the interaction of various sugars with boronic acid substituents on the complexed ligands.[26] Topologically chiral copper(I) catenates have been prepared with complete or partial resolution, where inversion of the copper configuration in the catenate is not possible.[27] A topologically chiral dicopper(I) trefoil knot (prepared by cyclization of a double-stranded, dimetal helicate) spontaneously resolves on crystallization,[28] and a similar dicopper(I) knot was resolved by fractional crystallization using a chiral counterion.[29] An oligo(2-ethynylpyridine) containing the (*D*)- or (*L*)-menthyloxy substituent combines with copper(I) to diastereoselectively self-assemble the enantiomers of a triple-stranded tetracopper(I) helicate.[30]

A detailed NMR characterization of double-stranded, dicopper(I) and disilver(I) complexes with bis(bidentate) Schiff-base ligands has been reported.[31] The complexes $[M_2L_2](CF_3SO_3)_2$ [M = Cu(I), Ag(I); L = **1a**,**b**] were prepared in high yields and crystallized as the racemates. A substituent effect on the rate of intermolecular exchange of silver(I) ions was observed, whereby the disilver(I) complex with the methyl-substituted ligand had a lower rate of exchange than the complex with the unsubstituted ligand. The disilver(I) complexes were found to be more labile than the corresponding dicopper(I) complexes.

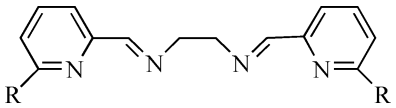

1a R = H
1b R = Me
1c R = *i*-Pr

Here, we present details of the preparation of double-stranded, dicopper(I) and disilver(I) helicates from the simple achiral Schiff-base ligands **1**, the kinetics of helicate racemization, and the second-order asymmetric transformation of a dicopper(I) helicate. The synthesis and structural characterization of (*R**,*R**)-(±)-$[Ag_2(\mathbf{1a})_2](BF_4)_2$ was previously reported by us.[32,33]

Results and Discussion

Preparation of Ligands. The route to 6-isopropyl-2-pyridinecarboxaldehyde (**5**) is given in Scheme 1 and follows modified literature procedures. The overall yield of **5** from isobutyryl chloride was ca. 10%. The syntheses of the pyridines **3**−**5** have not previously been published. The Schiff bases **1a**−**c** were prepared in good yields by the condensations in ethanol of 1,2-diaminoethane with 2 equiv of 2-pyridinecarboxaldehyde, 6-methyl-2-pyridinecarboxaldehyde, and 6-isopropyl-2-pyridinecarboxaldehyde (**5**), respectively. The ligands are air-stable solids and are stable in chloroform-d_1 for at least 1 month but decompose slowly in acetone-d_6 over 6 days (**1a**) or 11 days (**1b**,**c**).

Preparation of Complexes. The double-stranded, dicopper(I) and disilver(I) helicates containing **1a**−**c** were prepared in high yields as the hexafluorophosphate salts by reactions of the ligands with tetrakis(acetonitrile)copper(I) hexafluorophosphate or silver(I) hexafluorophosphate in acetonitrile (Scheme 2). The helicate salts crystallized on the addition of diethyl ether to the reaction mixtures. The complexes, (*R**,*R**)-(±)-$[Cu_2L_2](PF_6)_2$ (L = **1a**−**c**) were isolated as very dark orange-red, air-stable crystals, and the melting points were 256 °C (dec), 262 °C (dec), and 264 °C (dec), respectively. The complexes (*R**,*R**)-(±)-$[Ag_2L_2](PF_6)_2$ (L = **1a**−**c**) were obtained as yellow (**1a**) or cream (**1b**,**c**) crystals that decomposed at temperatures lower than their copper(I) analogues, viz. 219 °C (**1a**), 207 °C (**1b**), and 218 °C (**1c**).

Crystal and Molecular Structures of (*R,*R**)-(±)-$[M_2L_2](PF_6)_2$.** The double-stranded, dinuclear metal helicates crystallized as the racemates, (*R**,*R**)-(±)-$[M_2L_2](PF_6)_2$ [M = Cu(I), Ag(I); L = **1a**−**c**]. Crystal and molecular structures were obtained for the complexes (*R**,*R**)-(±)-$[Cu_2(\mathbf{1a})_2](PF_6)_2$, (*R**,*R**)-(±)-$[Cu_2(\mathbf{1c})_2](PF_6)_2$, and (*R**,*R**)-(±)-$[Ag_2(\mathbf{1c})_2](PF_6)_2$. Crystallographic data and experimental details for the three complexes are given in Table 1. Selected

(26) Yamamoto, M.; Takeuchi, M.; Shinkai, S.; Tani, F.; Naruta, Y. *J. Chem. Soc., Perkin Trans. 2* **2000**, 9. Yamamoto, M.; Takeuchi, M.; Shinkai, S. *Tetrahedron* **2002**, *58*, 7251.
(27) Kaida, Y.; Okamoto, Y.; Chambron, J.-C.; Mitchell, D. K.; Sauvage, J.-P. *Tetrahedron Lett.* **1993**, *34*, 1019.
(28) Dietrich-Buchecker, C. O.; Guilhem, J.; Pascard, C.; Sauvage, J.-P. *Angew. Chem., Int. Ed. Engl.* **1990**, *29*, 1154.
(29) Rapenne, G.; Dietrich-Buchecker, C.; Sauvage, J.-P. *J. Am. Chem. Soc.* **1996**, *118*, 10932. Dietrich-Buchecker, C.; Rapenne, G.; Sauvage, J.-P.; De Cian, A.; Fischer, J. *Chem.*—Eur. J. **1999**, *5*, 1432.
(30) Kawano, T.; Kato, T.; Du, C.-X.; Ueda, I. *Bull. Chem. Soc. Jpn* **2003**, *76*, 709.
(31) van Stein, G. C.; van Koten, G.; Vrieze, K.; Brevard, C. *Inorg. Chem.* **1984**, *23*, 4269.
(32) Bowyer, P. K.; Porter, K. A.; Rae, A. D.; Willis, A. C.; Wild, S. B. *J. Chem. Soc., Chem. Commun.* **1998**, 1153.
(33) The use of the relative configuration descriptors (*R**,*R**)-(±) and (*R**,*S**) for the racemic and meso diastereomers of the complexes, respectively, conforms with current Chemical Abstracts practice and IUPAC recommendations for analogous organic compounds.

Scheme 2

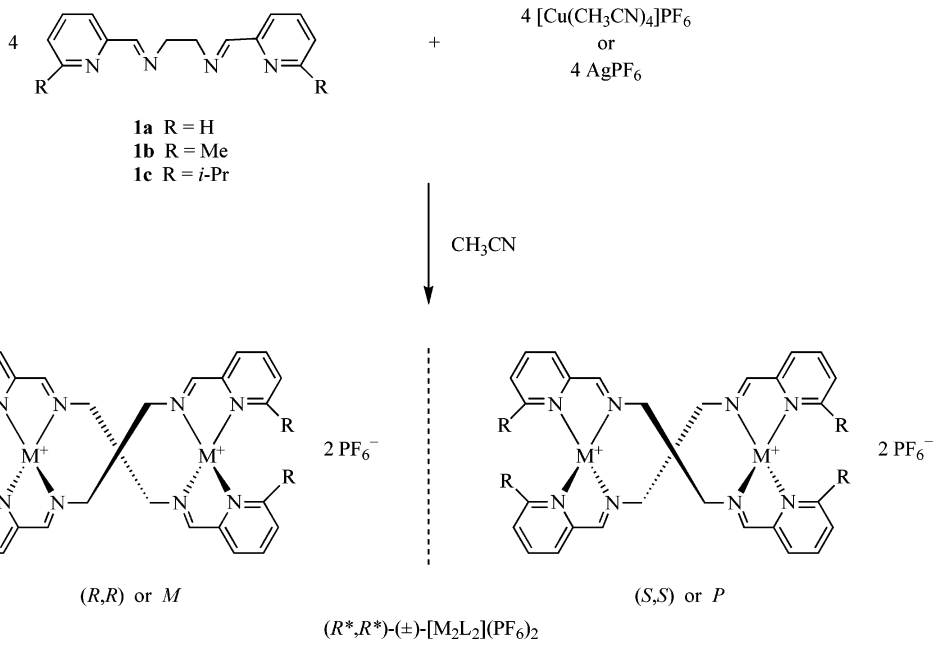

Table 1. Crystallographic Data and Experimental Parameters for the X-ray Structure Analyses

param	(*R**,*R**)-(±)-[Cu_2(**1a**)$_2$](PF_6)$_2$	(*R**,*R**)-(±)-[Cu_2(**1c**)$_2$](PF_6)$_2$	(*R**,*R**)-(±)-[Ag_2(**1c**)$_2$](PF_6)$_2$·CH_3CN	(*R*,*R*)-[Cu_2(**1c**)$_2$]{Δ-(−)-[As(cat)$_3$]}$_2$·CH_2Cl_2
molec formula	$C_{28}H_{28}Cu_2F_{12}N_8P_2$	$C_{40}H_{52}Cu_2F_{12}N_8P_2$	$C_{42}H_{55}Ag_2F_{12}N_9P_2$	$C_{77}H_{78}As_2Cl_2Cu_2N_8O_{12}$
fw	893.60	1061.92	1191.62	1655.35
cryst color, habit	red, irregular prism	red, prism	cream, block	brown, plate
space group	$P2_1/c$	$P2_1/c$	$P\bar{1}$	$P2_1$
cryst syst	monoclinic	monoclinic	triclinic	monoclinic
a, Å	14.9178(2)	17.9164(2)	11.2078(3)	12.3419(2)
b, Å	11.6683(2)	10.47810(10)	14.3947(5)	25.9815(4)
c, Å	21.4158(3)	26.2098(2)	16.2084(6)	12.4508(2)
α, deg			100.777(2)	
β, deg	109.9056(8)	106.8130(5)	92.512(2)	111.3325(7)
γ, deg			108.916(2)	
V, Å^3	3505.03(9)	4710.04(8)	2414.70(14)	3718.94(10)
Z	4	4	2	2
D_{calcd}, g cm^{-3}	1.693	1.497	1.639	1.478
cryst size, mm^3	0.30 × 0.30 × 0.10	0.32 × 0.16 × 0.13	0.17 × 0.15 × 0.06	0.29 × 0.16 × 0.04
μ, cm^{-1}	14.03	10.59	9.65	15.94
instrument	Nonius Kappa CCD	Nonius Kappa CCD	Nonius Kappa CCD	Nonius Kappa CCD
radiatn	Mo Kα	Mo Kα	Mo Kα	Mo Kα
no. unique reflcns	8021	12 680	8552	16 460
no. reflcns obsd	4095 ($I > 3\sigma(I)$)	6595 ($I > 3\sigma(I)$)	5333 ($I > 3\sigma(I)$)	10 430 ($I > 3\sigma(I)$)
θ range, deg	2.5−27.5	2.5−29.1	2.5−25.1	2.9−27.7
temp, K	200	200	200	200
struct refinement	CRYSTALS[68]	CRYSTALS[68]	CRYSTALS[68]/maXus[69]	CRYSTALS[68]/maXus[69]
final *R*, R_w	0.0268, 0.0304	0.0294, 0.0341	0.0531, 0.0622	0.0436, 0.0486

interatomic bond lengths and angles following the numbering scheme shown in Figure 1 are given in Table 2. The molecular structures of the cations are shown in Figures 2−4 for (*R**,*R**)-(±)-[Cu_2(**1a**)$_2$](PF_6)$_2$, (*R**,*R**)-(±)-[Cu_2(**1c**)$_2$](PF_6)$_2$, and (*R**,*R**)-(±)-[Ag_2(**1c**)$_2$](PF_6)$_2$, respectively.

The molecular structures of the cations of (*R**,*R**)-(±)-[Cu_2(**1a**)$_2$](PF_6)$_2$, (*R**,*R**)-(±)-[Cu_2(**1c**)$_2$](PF_6)$_2$, and (*R**,*R**)-(±)-[Ag_2(**1c**)$_2$](PF_6)$_2$ are similar to those reported for related dinuclear complexes of copper(I) and silver(I) with bis(bidentate) Schiff-base ligands.[31,34,35] The two metal centers in the complexes are of the same configuration, either (*R*,*R*) or (*S*,*S*), hence the relative descriptor (*R**,*R**)-(±).[33] The (*R*,*S*) or (*R**,*S**)[33] diastereomers of the complexes were not observed in the solid state. The overall helicity (*P* or *M*) of the cation corresponds to the metal configurations as follows: (*R*,*R*) ≡ *M*, and (*S*,*S*) ≡ *P*.[36]

The structural determinations of (*R**,*R**)-(±)-[Cu_2(**1a**)$_2$](PF_6)$_2$ and (*R**,*R**)-((±))-[Cu_2(**1c**)$_2$](PF_6)$_2$ revealed four

(34) van Stein, G. C.; van der Poel, H.; van Koten, G.; Spek, A. L.; Duisenberg, A. J. M.; Pregosin, P. S. *J. Chem. Soc., Chem. Commun.* **1980**, 1016. van Stein, G. C.; van Koten, G.; Vrieze, K.; Brevard, C.; Spek, A. L. *J. Am. Chem. Soc.* **1984**, *106*, 4486. van Stein, G. C.; van Koten, G.; Passenier, H.; Steinebach, O.; Vrieze, K. *Inorg. Chim. Acta* **1984**, *89*, 79. van Stein, G. C.; van Koten, G.; Blank, F.; Taylor, L. C.; Vrieze, K.; Spek, A. L.; Duisenberg, A. J. M.; Schreurs, A. M. M.; Kojiæ-Prodiæ, B.; Brevard, C. *Inorg. Chim. Acta* **1985**, *98*, 107.
(35) Lange, J.; Elias, H.; Paulus, H.; Müller, J.; Weser, U. *Inorg. Chem.* **2000**, *39*, 3342.
(36) Eliel, E. L.; Wilen, S. H.; Mander, L. N. *Stereochemistry of Organic Compounds*; John Wiley & Sons: New York, 1994; Chapter 14, p 1121.

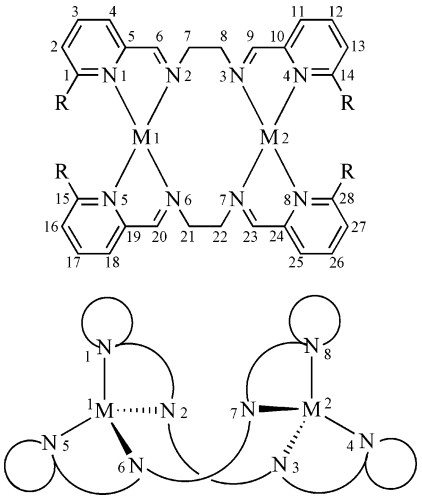

Figure 1. Numbering scheme used for crystal structure determinations of (*R**,*R**)-(±)-$[M_2L_2](PF_6)_2$ [M = Cu(I), L = **1a**,**c**; M = Ag(I), L = **1c**].

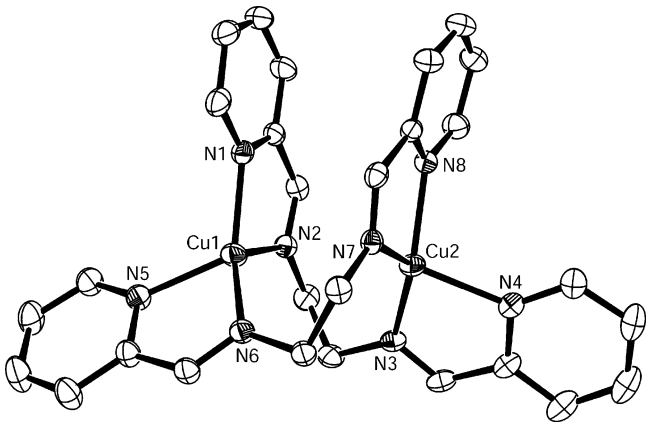

Figure 2. Molecular structure of the cation (*R**,*R**)-(±)-$[Cu_2(\mathbf{1a})_2]^{2+}$ ((*R*,*R*) enantiomer shown).

cations and associated anions in the unit cell—two of the (*R*,*R*) configuration (*M* helix) and two of the (*S*,*S*) configuration (*P* helix). The two molecules of each enantiomer are related by a screw axis. An inversion center and a glide plane

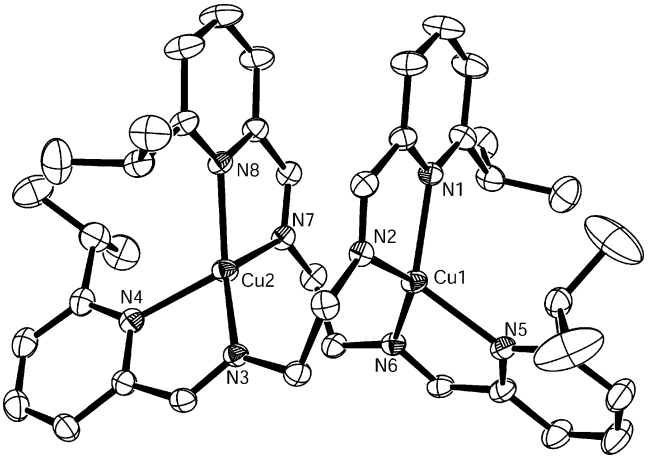

Figure 3. Molecular structure of the cation (*R**,*R**)-(±)-$[Cu_2(\mathbf{1c})_2]^{2+}$ ((*R*,*R*) enantiomer shown).

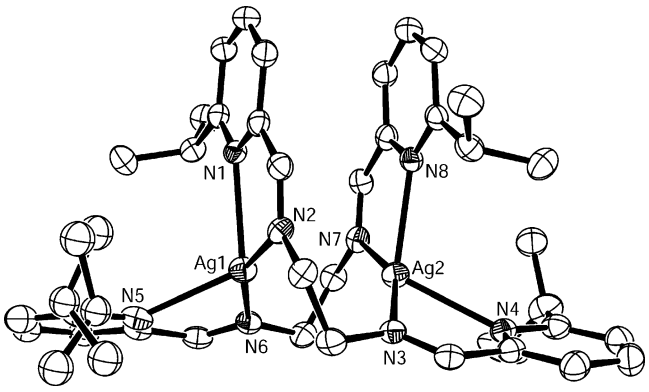

Figure 4. Molecular structure of the cation (*R**,*R**)-(±)-$[Ag_2(\mathbf{1c})_2]^{2+}$ ((*S*,*S*) enantiomer shown).

relate the two molecules of one enantiomer to the other enantiomer. The structural determination of (*R**,*R**)-((±))-$[Ag_2(\mathbf{1c})_2](PF_6)_2$ revealed two cations and associated hexafluorophosphate ions in the unit cell: one cation of the (*R*,*R*) configuration (*M* helix) and one of the (*S*,*S*) configuration (*P* helix). The two enantiomers in the lattice are related by

Table 2. Selected Bond Distances (Å) and Bond Angles (deg) for the Cations (*R**,*R**)-(±)-$[M_2L_2]^{2+}$

param	(*R**,*R**)-(±)-$[Cu_2(\mathbf{1a})_2](PF_6)_2$	(*R**,*R**)-(±)-$[Cu_2(\mathbf{1c})_2](PF_6)_2$	(*R**,*R**)-(±)-$[Ag_2(\mathbf{1c})_2](PF_6)_2{\cdot}CH_3CN$	(*R*,*R*)-$[Cu_2(\mathbf{1c})_2]$\{Δ-(−)-$[As(cat)_3]\}_2{\cdot}CH_2Cl_2$
M1−N1	2.025(2)	2.069(2)	2.446(5)	2.086(4)
M1−N2	2.028(2)	2.010(2)	2.256(5)	2.015(4)
M1−N5	2.071(2)	2.085(2)	2.468(6)	2.083(4)
M1−N6	2.002(2)	1.999(2)	2.240(5)	2.002(4)
M2−N3	1.993(2)	2.006(2)	2.237(5)	2.015(4)
M2−N4	2.109(2)	2.071(2)	2.508(5)	2.059(5)
M2−N7	2.024(2)	2.020(2)	2.263(5)	2.020(4)
M2−N8	2.045(2)	2.068(2)	2.419(5)	2.072(5)
M1−M2	3.513(1)	3.598(1)	3.1706(7)	3.6631(9)
N1−M1−N2	81.69(9)	81.29(7)	72.33(17)	80.84(17)
N1−M1−N5	118.69(9)	118.22(8)	110.08(17)	111.87(16)
N1−M1−N6	136.50(9)	127.60(7)	119.51(17)	119.49(17)
N2−M1−N5	114.63(9)	117.67(12)	125.99(18)	133.91(16)
N2−M1−N6	127.12(10)	134.57(8)	155.81(19)	132.74(17)
N5−M1−N6	81.48(9)	81.83(8)	72.23(19)	80.97(16)
N3−M2−N4	80.77(10)	81.17(8)	71.92(7)	81.07(18)
N3−M2−N7	129.90(9)	131.71(7)	155.93(18)	129.62(18)
N3−M2−N8	140.96(9)	130.29(7)	95.96(11)	123.36(19)
N4−M2−N7	120.17(9)	119.64(8)	125.31(17)	128.00(17)
N4−M2−N8	104.59(9)	117.00(7)	109.24(16)	118.31(18)
N7−M2−N8	81.45(9)	81.52(7)	72.80(18)	81.96(18)

a center of inversion. When viewed down the *a* or the *c* axis, the molecules pack in columns of alternating enantiomers. There was disorder of the isopropyl groups of the cation and disorder of the anions in the lattice of this compound.

For (*R**,*R**)-((±))-$[Cu_2(\mathbf{1a})_2](PF_6)_2$ and (*R**,*R**)-((±))-$[Cu_2(\mathbf{1c})_2](PF_6)_2$, the Cu−N distances are in the range 1.99−2.11 Å, which are the lengths typical of imine-N−Cu bonds. The Ag−*N* bond distances in (*R**,*R**)-((±))-$[Ag_2(\mathbf{1c})_2](PF_6)_2$ lie in the range 2.24−2.51 Å. The pyridyl-*N*−Ag distances are, on average, 0.21 Å longer than the azomethine-*N*−Ag distances in (*R**,*R**)-((±))-$[Ag_2(\mathbf{1c})_2](PF_6)_2$. The coordination geometry of the copper(I) and silver(I) centers in the complexes is distorted tetrahedral. For all three complexes, the N_p-M-N_i angles (where N_p and N_i are the respective pyridine- and imine-*N* atoms in the chelate ring) are significantly smaller than the other N−M−N angles. The angles N_p-M-N_i for the four chelate rings in both copper(I) complexes lie in the range 80.7−81.83 Å. In (*R**,*R**)-((±))-$[Ag_2(\mathbf{1c})_2](PF_6)_2$, the N_p-M-N_i angles are smaller (71.92−72.8 Å) because of the longer Ag−N bonds. The "outer" bond angles $N_{pa}-M-N_{pb}$ between the two pyridyl nitrogen atoms (N1−M1−N5 and N4−M2−N8) are smaller than the "inner" angles $N_{ia}-M-N_{ib}$ for the imine nitrogen atoms of the central 10-membered ring (N2−M1−N6 and N3−M2−N7). This difference is particularly noticeable in the structure of (*R**,*R**)-((±))-$[Ag_2(\mathbf{1c})_2](PF_6)_2$, which has $N_{pa}-M-N_{pb}$ angles of 110° and $N_{ia}-M-N_{ib}$ angles of 156°.

Five rings result from the formation of the double-stranded, dimetal helicates: two 5-membered chelate rings around each metal and a central 10-membered ring containing the two metal ions. The 5-membered rings are almost planar. The conformations of the central 10-membered rings in the helicates cannot be compared directly with those available to cyclodecane[37,38] because the four, planar sp^2-hybridized nitrogen atoms in the ring limit the number of possible conformations. The chirality of the central 10-membered ring can be viewed in terms of the helicity associated with the 1,2-ethano backbone groups. The twisting of the $-CH_2-CH_2-$ bonds leads to three general conformations possible for the helicates. In a simplistic sense, each carbon−carbon bond of the ethano group can be parallel or perpendicular to the overall helicity of the cation. The three conformations of the central ring can be described as $\delta\delta$, $\lambda\lambda$, and $\delta\lambda$, where each δ/λ refers to the local helicity of each $-CH_2-CH_2-$ bond. The three stylized structures showing the conformations for the (*R*,*R*) or *M* enantiomer of the dinuclear complex are shown in Figure 5. The *R*-$\delta\delta$-*R* conformer (and its enantiomer *S*-$\lambda\lambda$-*S*) of D_2 symmetry is termed a side-by-side helicate as each ligand strand sits on one side of the metal−metal axis. In the *R*-$\lambda\lambda$-*R* conformer, however, the ligand strands wrap themselves along and around the metal−metal axis, making the structure reminiscent of a D_2 double α-helix. The central 10-membered ring in the structure adopts

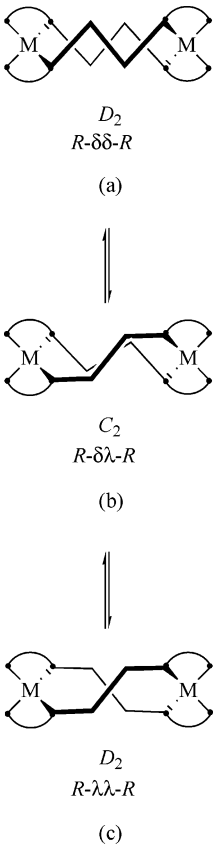

Figure 5. Schematic side elevations of the three possible conformations of the cation (*R*,*R*)-$[M_2L_2]^{2+}$.

the unsymmetrical conformation ($\delta\lambda$) in the solid, however, wherein each half of each ligand is nonequivalent. The structure found in the solid state has one C_2 axis: the change in conformation of the central 10-membered ring from $\delta\delta$ (or $\lambda\lambda$) to $\delta\lambda$ leads to the loss of two C_2 axes in the cation.

As mentioned earlier, related helicates also crystallize with lower symmetry cations.[31,34,35] The reason for the low symmetry preference in the solid state is unclear, but there is evidence for intramolecular stacking between one pair of adjacent pyridine rings of separate ligand strands. The nonbonding metal−metal distances are 3.51 Å for (*R**,*R**)-((±))-$[Cu_2(\mathbf{1a})_2](PF_6)_2$, 3.60 Å for (*R**,*R**)-((±))-$[Cu_2(\mathbf{1c})_2](PF_6)_2$, and 3.17 Å for (*R**,*R**)-((±))-$[Ag_2(\mathbf{1c})_2](PF_6)_2$. There do not appear to be cuprophilic or argentophilic interactions in the complexes. For the helicates (*R**,*R**)-((±))-$[Cu_2(\mathbf{1a})_2](PF_6)_2$, (*R**,*R**)-((±))-$[Cu_2(\mathbf{1c})_2](PF_6)_2$, and (*R**,*R**)-((±))-$[Ag_2(\mathbf{1c})_2](PF_6)_2$, the crystal packing diagrams do not indicate any π-stacking interactions between adjacent molecules, even though the cations do tend to pack "back-to-back" when viewed along certain axes.

Solution Properties. (a) NMR Spectroscopy. The ^1H and ^{13}C NMR spectra of the six complexes (*R**,*R**)-((±))-$[M_2L_2](PF_6)_2$ [M = Cu(I), Ag(I); L = **1a**−**c**] were recorded in various solvents at 20 °C. The spectra were similar for all combinations of the three ligands and two metal ions. It should be noted that, in solution, the double-stranded dinuclear cations adopt highly symmetrical D_2 structures and do not retain the C_2 structures observed in the solid state (Figure 5). If the C_2 structures were present in solution, the

(37) Hendrickson, J. B. *J. Am. Chem. Soc.* **1967**, *89*, 7047. Dunitz, J. D. In *Perspectives in Structural Chemistry*; Dunitz, J. D., Ibers, J. A., Eds.; John Wiley & Sons: New York, 1968; Vol. II, pp 1−70.
(38) Hilderbrandt, R. L.; Wieser, J. D.; Montgomery, L. K. *J. Am. Chem. Soc.* **1973**, *95*, 8598. Pawar, D. M.; Smith, S. V.; Mark, H. L.; Odom, R. M.; Noe, E. A. *J. Am. Chem. Soc.* **1998**, *120*, 10715.

NMR spectra would show two sets of peaks corresponding to the nonequivalent halves of the ligands in each cation (Figure 1).[31,34] The ^{1}H and ^{13}C NMR spectra of the complexes indicate that the helicate cation has a highly symmetrical or averaged structure in solution since there is only one set of peaks for the ligand strands in each case.

The most notable effect upon coordination of the ligand is the change in chemical shift that occurs for the azomethine protons (N═C*H*), which shift downfield by about 0.6 ppm in all of the complexes. For the free ligand **1a**, the azomethine-*H* resonance occurs upfield of *H*C-6 of the pyridine ring (δ 8.36 for N═C*H* vs δ 8.58 for *H*C-6 in acetone-d_6) but downfield when the ligand is coordinated to copper(I) (δ 8.77 for N═C*H* vs δ 8.43 for *H*C-6) or silver-(I) (δ 8.86 for N═C*H* vs. δ 8.46 for *H*C-6).

Stabilities of Helicates in Solution. Acetone-d_6, acetonitrile-d_3, nitromethane-d_3, and dichloromethane-d_2 solutions of the three copper(I) helicates (ca. 2×10^{-5} M) under atmospheric conditions were generally stable for at least 1 month at room temperature. The exceptions were (*R**,*R**)-((±))-[Cu_2(**1a**)$_2$](PF_6)$_2$ in acetone-d_6 and nitromethane-d_3 and (*R**,*R**)-((±))-[Cu_2(**1b**)$_2$](PF_6)$_2$ in acetone-d_6. Decomposition of these samples was apparent both from the NMR spectra and the appearance of the solutions in each case. The helicate (*R**,*R**)-((±))-[Cu_2(**1a**)$_2$](PF_6)$_2$ completely decomposed after 1 month in nitromethane-d_3. In acetonitrile-d_3 and dichloromethane-d_2 solutions, the complex was stable for at least 2 and 1 month, respectively. Acetone-d_6 and acetonitrile-d_3 solutions of the three silver(I) helicates (ca. 2×10^{-5} M) were stable for at least 1 month at room temperature. Indeed, in acetone-d_6, the silver(I) helicates were less susceptible to decomposition than the corresponding copper(I) helicates.

Proton−Silver Coupling. The azomethine-*H* resonances occur as sharp singlets in the three copper(I) helicates, as a broad singlet in (*R**,*R**)-((±))-[Ag_2(**1a**)$_2$](PF_6)$_2$ and as doublets in (*R**,*R**)-((±))-[Ag_2(**1b**)$_2$](PF_6)$_2$ and (*R**,*R**)-((±))-[Ag_2(**1c**)$_2$](PF_6)$_2$. This multiplicity for the azomethine-*H* resonance in the silver(I) helicates is due to a three-bond, proton−silver coupling, $^3J_{AgH} = 8.5$ and 8.8 Hz for (*R**,*R**)-((±))-[Ag_2(**1b**)$_2$](PF_6)$_2$ and (*R**,*R**)-((±))-[Ag_2(**1c**)$_2$]-(PF_6)$_2$, respectively. There are two isotopes of silver with spin $I = 1/2$, each of approximately 50% natural abundance: ^{107}Ag (51.84%); ^{109}Ag (48.16%). Three-bond, proton−silver coupling is typically observed for the azomethine-type systems H−C═N→Ag.[39]

Diastereotopicity of the Methylene Protons and Isopropyl-Me Groups. The ^{1}H NMR spectra of the helicates should show the −CH_2−CH2− protons as AA′BB′ spin systems,[13,40] yet rarely were multiplets observed at room temperature. Of the six complexes, only (*R**,*R**)-((±))-[Cu_2-(**1a**)$_2$](PF_6)$_2$ showed the methylene protons as multiplets in the following three solvents at 20 °C: δ 4.40 ppm (acetone-d_6); 4.28 (dichloromethane-d_2); 4.38 (nitromethane-d_3, partly obscured by residual solvent peak). In acetonitrile-d_3, a sharp singlet was observed for the methylene protons of the complex. For the five other complexes in the various solvents, the methylene protons occurred as sharp singlets in the region δ 4.15−4.45 ppm. Lowering of the temperature (−80 to −90 °C) of the acetone-d_6 solutions of the complexes led to broadening of the methylene resonances in the ^{1}H NMR spectra. The apparent lack of diastereotopicity in the ^{1}H NMR spectra for the methylene protons suggests that the resonances are accidentally isochronous, since the protons are formally diastereotopic in the (*R**,*R**)-((±)) and (*R**,*S**) forms of the complex.

The complexes (*R**,*R**)-((±))-[Cu_2(**1c**)$_2$](PF_6)$_2$ and (*R**,*R**)-((±))-[Ag_2(**1c**)$_2$](PF_6)$_2$ contain another set of diastereotopic groups—the methyl groups of the isopropyl groups.[10] The ^{1}H NMR spectrum of the free ligand **1c** contains one doublet corresponding to equivalent methyl groups of the isopropyl group. On complexation to a tetrahedral metal center, the isopropyl-*Me* groups in the bis(bidentate) ligand become diastereotopic because of the chirality of the complex and resonate as two doublets in the ^{1}H NMR spectrum. Cooling a sample of (*R**,*R**)-((±))-[Cu_2(**1c**)$_2$](PF_6)$_2$ to −80 °C did not lead to broadening of the methylene resonance. At the same time, the isopropyl-*Me* resonances remained as two sharp, well-defined doublets, separated by ca. 0.52 ppm.

NMR Spectra in the Presence of a Chiral Lanthanide Shift Reagent. On addition of (+)-Eu(hfc)$_3$ (1 equiv) to a CD_2Cl_2 solution of (*R**,*R**)-((±))-[Cu_2(**1c**)$_2$](PF_6)$_2$, there is a large induced downfield shift as well as separation of the proton peaks corresponding to the diastereomers of the chiral LSR-helicate complex.[13,41−43] The isopropyl-*Me*, isopropyl-C*H*Me_2, and pyridine-*H* resonances do not show large diastereotopic splittings. Indeed, the *H*C-4 peak of the pyridine rings is not split, although it is shifted (δ 7.95 to 8.08 ppm). The methylene- and azomethine-*H* resonances show the greatest diastereotopic splittings. The two azomethine-*H* signals corresponding to (*R*,*R*)-[Cu_2(**1c**)$_2$](PF_6)$_2$−(+)-Eu(hfc)$_3$ and (*S*,*S*)-[Cu_2(**1c**)$_2$](PF_6)$_2$−(+)-Eu(hfc)$_3$ occur at δ 8.55 and 8.66 ppm (assignment arbitrary), and have baseline separation (Figure 6). The methylene resonances in the spectrum appear as two multiplets at δ 4.39 (broad, unresolved) and δ 4.60 (pseudo quartet with $^2J_{AB} = {}^2J_{A'B'} =$ 11.8 Hz). Lanthanide shift reagents can cause accidentally isochronous resonances to become anisochronous,[42] which is the reason two multiplets were observed for the methylene resonances in this system rather than two singlets. After 1 week, the ^{1}H NMR spectrum of (*R**,*R**)-((±))-[Cu_2(**1c**)$_2$]-(PF_6)$_2$ with (+)-Eu(hfc)$_3$ in dichloromethane-d_2 solution was essentially unchanged. A slight broadening of the LSR peaks was evident, but the ratio of the enantiomers of (*R**,*R**)-((±))-[Cu_2(**1c**)$_2$](PF_6)$_2$ remained 1:1. Indeed, the ^{1}H NMR spectrum of (*R**,*R**)-((±))-[Cu_2(**1c**)$_2$](PF_6)$_2$ with (+)-Eu(hfc)$_3$ did not change over 1 month at 23 °C.

When 2 equiv of (+)-Eu(hfc)$_3$ is added to (*R**,*R**)-((±))-[Cu_2(**1c**)$_2$](PF_6)$_2$, the ^{1}H NMR spectrum in dichloromethane-

(39) Granger, P. In *Transition Metal Nuclear Magnetic Resonance*; Pregosin, P. S., Ed.; Elsevier: Amsterdam, 1991; pp 264−346.
(40) Piguet, C.; Bünzli, J.-C. G.; Bernardinelli, G.; Hopfgartner, G.; Williams, A. F. *J. Am. Chem. Soc.* **1993**, *115*, 8197.
(41) Lehn, J.-M.; Rigault, A. *Angew. Chem., Int. Ed. Engl.* **1988**, *27*, 1095.
(42) Wenzel, T. J. *NMR Shift Reagents*; CRC Press: Boca Raton, FL, 1987; pp 127−154.
(43) Thompson, A.; Dolphin, D. *Org. Lett.* **2000**, *2*, 1315.

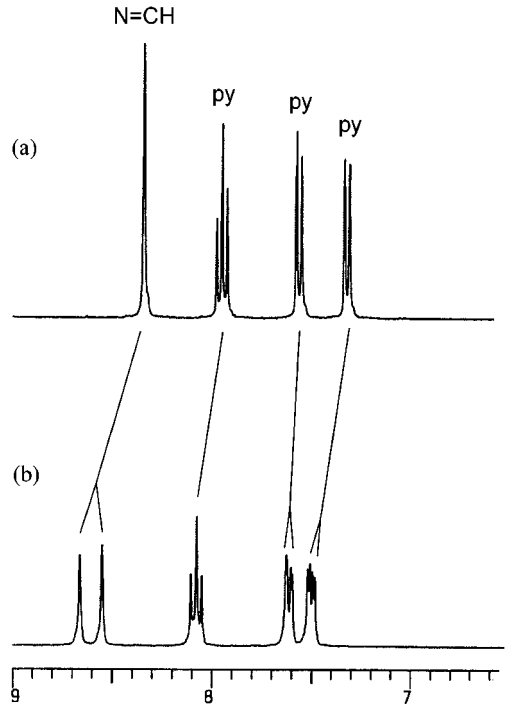

Figure 6. ^{1}H NMR spectra (CD_2Cl_2, 20 °C, 300 MHz) in the azomethine-*H* and py*H* regions of (a) (*R**,*R**)-(±)-$[Cu_2(\mathbf{1c})_2](PF_6)_2$ and (b) (*R**,*R**)-(±)-$[Cu_2(\mathbf{1c})_2](PF_6)_2$ in the presence of (+)-Eu(hfc)$_3$ (1 equiv).

d_2 does not show a greater induced shift or diastereotopic splitting compared to the addition of 1 equiv of the chiral LSR. Indeed, the pyridyl-*H*'s no longer show diastereotopic splitting and all of the resonances are slightly upfield of those observed with 1 equiv of (+)-Eu(hfc)$_3$. The splitting observed for the azomethine-*H* resonance is slightly smaller at 0.106 ppm for 2 equiv of (+)-Eu(hfc)$_3$ (cf. 0.112 ppm for 1 equiv). Even though there are two hexafluorophosphate anions for each cation, the effect of the chiral LSR is greater when the ratio of the anion to the LSR is 2:1 rather than 1:1. It is surprising that the chiral LSR induced such a large chemical shift difference between the two possible diastereomers of the hexafluorophosphate salt of the complexes. The literature suggests that a small, nucleophilic anion (unlike the hexafluorophosphate) is necessary for the interaction of the chiral LSR with the anion in order that ion-pairing can occur.[44]

Lanthanide shift reagent investigations were also performed with the helicates (*R**,*R**)-((±))-$[Cu_2(\mathbf{1a})_2](PF_6)_2$, (*R**,*R**)-((±))-$[Cu_2(\mathbf{1b})_2](PF_6)_2$, and (*R**,*R**)-((±))-$[Ag_2(\mathbf{1c})_2](PF_6)_2$. Helicate (*R**,*R**)-((±))-$[Cu_2(\mathbf{1c})_2](PF_6)_2$ with (+)-Eu(hfc)$_3$ in dichloromethane-d_2 gives sharp, shifted resonances with diastereotopic splittings, yet (*R**,*R**)-((±))-$[Cu_2(\mathbf{1b})_2](PF_6)_2$ with (+)-Eu(hfc)$_3$ gives broad, shifted resonances with diastereotopic splitting and the chiral LSR had no effect on the ^{1}H NMR spectrum of (*R**,*R**)-((±))-$[Cu_2(\mathbf{1a})_2](PF_6)_2$. These results suggest that a bulky substituent at C-6 of the pyridine ring lends greater configurational stability to the helicate.

For the helicate (*R**,*R**)-((±))-$[Ag_2(\mathbf{1c})_2](PF_6)_2$, the ^{1}H NMR spectrum in the presence of (+)-Eu(hfc)$_3$ (1 equiv) in dichloromethane-d_2 shows a diastereotopic splitting for some protons but no induced shift. The methylene resonance (δ 4.25 ppm in (*R**,*R**)-((±))-$[Ag_2(\mathbf{1c})_2](PF_6)_2$ becomes two overlapping singlets at δ 4.27 and 4.31 ppm in the presence of the chiral LSR.

The investigations have shown that the enantiomeric excess (ee) of the helicate (*R**,*R**)-((±))-$[Cu_2(\mathbf{1c})_2](PF_6)_2$ can be determined by ^{1}H NMR spectroscopy in the presence of (+)-Eu(hfc)$_3$ in dichloromethane-d_2.

(b) Conductivities. The molecular complexity (z) of a salt of formula $[ML_n]_z[X]_{yz}$ cannot be determined by measuring the conductivity of its solution at a single concentration, since the molar conductivity (Λ_m) and the equivalent conductivity (Λ_{eq}) are not directly related to z.[45] The change in equivalent conductance with concentration is, however, directly related to the molecular complexity. The Onsager law, $\Lambda_{eq} = \Lambda_0 - A\sqrt{(C_{eq})}$, can be used to determine the type of electrolyte. A plot of Λ_{eq} against the square root of equivalent concentration (C_{eq}) gives a straight line of slope A. Comparisons of A with values for known electrolytes under similar conditions can then be used to indicate the electrolyte type of the complex in question.

The conductances of $10^{-2}-10^{-4}$ M solutions of the six complexes (*R**,*R**)-((±))-$[M_2L_2](PF_6)_2$ [M = Cu(I), Ag(I); L = **1a**−**c**] in nitromethane at 24 °C were determined. The values of A (1350−1520 S cm^2 L$^{1/2}$ equiv$^{-3/2}$), which were determined by plotting Λ_{eq} against $\sqrt{C_{eq}}$, correspond to 2:1 electrolytes in solution. From these data, it is apparent that the complexes are di-univalent electrolytes (helicates) in this solvent. Values of A of 1324 and 1538 S cm^2 L$^{1/2}$ equiv$^{-3/2}$ have been reported for certain dicopper(I) helicates in DMF.[46]

Kinetics of Intermolecular Ligand Exchange and Intramolecular Inversion. Racemization of the helicates, (*R*,*R*) ⇌ (*S*,*S*) or *M* ⇌ *P*, can occur by intermolecular or intramolecular processes, and given the simple ^{1}H NMR spectra observed, the kinetics of these processes can be investigated by NMR spectroscopy. The ^{1}H NMR spectra of the helicates indicated that the complexes were stable for lengthy periods in solution, which allowed experiments involving ligand exchange or redistribution to be conducted without concern for decomposition.

Ligand redistribution between enantiomers via an intermolecular process involves complete dissociation of one ligand from the complex. In all, eight metal−nitrogen bonds must be broken and eight similar bonds formed for intermolecular ligand exchange. Intramolecular processes can involve either a twist mechanism (inversion of each tetrahedral metal stereocenter via a square plane) or dissociation of some, but not all, of the metal−nitrogen bonds from each ligand in the complex. Intramolecular inversion in complexes is best investigated by the coalescence of diastereotopic groups in ^{1}H NMR spectra, hence the choice of the isopropyl substituent on the ligand in this work.

(1) Intermolecular Ligand Exchange. The rate of intermolecular ligand exchange was investigated by using

(44) Barton, J. K.; Nowick, J. S. *J. Chem. Soc., Chem. Commun.* **1984**, 1650.

(45) Feltham, R. D.; Hayter, R. G. *J. Chem. Soc.* **1964**, 4587.

(46) Rüttimann, S.; Piguet, C.; Bernardinelli, G.; Bocquet, B.; Williams, A. F. *J. Am. Chem. Soc.* **1992**, *114*, 4230.

Table 3. Kinetics of Intermolecular Ligand Exchange between (*R**,*R**)-(±)-$[M_2(L1)_2](PF_6)_2$ (**A**) and (*R**,*R**)-(±)-$[M_2(L2)_2](PF_6)_2$ (**B**) To Give (*R**,*R**)-(±)-$[M_2(L1)(L2)](PF_6)_2$ (**C**) from ^{1}H NMR Spectra

run	metal	ligands (L1 + L2)	solvent	temp (°C)	$t_{1/2}$	k (s^{-1})	ratio[c] (**A** + **B**):**C**
1[a]	Cu	**1a** + **1b**	$(CD_3)_2CO$	23	110 h	1.8×10^{-6}	1:1
2[b]	Cu	**1a** + **1b**	$(CD_3)_2CO$	45	2 h	9.3×10^{-5}	1:1
3[b]	Cu	**1a** + **1b**	$(CD_3)_2CO$	54	0.9 h	2.1×10^{-4}	1:1
4[b]	Cu	**1a** + **1b**	CD_3CN	25	<5 min	$>2 \times 10^{-3}$	1:1
5[a]	Cu	**1b** + **1c**	$(CD_3)_2CO$	23	120 h	1.6×10^{-6}	0.75:1
6[a]	Cu	**1b** + **1c**	CD_3CN	23	<5 min	$>2 \times 10^{-3}$	0.75:1
7[a]	Cu	**1b** + **1c**	CD_2Cl_2	23	40 h	4.9×10^{-6}	0.75:1
8[b]	Ag	**1a** + **1b**	$(CD_3)_2CO$	25	<3 min	$>4 \times 10^{-3}$	1:1
9[b]	Ag	**1a** + **1b**	CD_3CN	25	<3 min	$>4 \times 10^{-3}$	1:1
10[b]	Ag	**1b** + **1c**	$(CD_3)_2CO$	25	<5 min	$>2 \times 10^{-3}$	0.75:1
11[a]	Ag	**1b** + **1c**	CD_3CN	23	<5 min	$>2 \times 10^{-3}$	1:1

[a] Spectra recorded at 300 MHz. [b] Spectra recorded at 500 MHz. [c] Ratios estimated to be within 5% on the basis of integrals for azomethine (N=C*H*) protons in ^{1}H NMR spectra.

two differently substituted helicates. Reaction of helicate **A** with helicate **B** gives 2 equiv of the crossover helicate **C** (eq 1).

$$\underset{\mathbf{A}}{[M_2(L1)_2](PF_6)_2} + \underset{\mathbf{B}}{[M_2(L2)_2](PF_6)_2} \rightleftharpoons 2\underset{\mathbf{C}}{[M_2(L1)(L2)](PF_6)_2} \quad (1)$$

The ratios of the reactant helicates (**A** plus **B**) to the product helicate (**C**) for the intermolecular ligand exchange reactions were determined by integration of the azomethine-*H* resonances. The azomethine-*H* resonances for the components of the mixture have baseline separations when using helicates with different substituents at the C-6 position of the pyridine ring. Integration ratios for the azomethine-*H* atoms for **A**−**C** were checked by comparison with the integration ratios of other peaks, such as the methyl resonances, providing they also had baseline separation.

The general procedure for the ligand exchange experiments was to dissolve equimolar amounts of helicate **A** and helicate **B** (ca. 0.02 g of each) in the desired solvent (0.7 mL). The first spectrum of the sample was obtained within 5 min of the addition of the solvent. ^{1}H NMR spectra were recorded on Varian Inova 500 MHz or Varian Gemini 300 MHz spectrometers, as indicated in Table 3.

(a) Treatment of Kinetic Data for Intermolecular Ligand Exchange. The kinetics of ligand exchange between mononuclear complexes containing two bidentate ligands have been reported as second-order reversible reactions:[47]

$$M_2(L1)_2 + M_2(L2)_2 \underset{k_{-1}}{\overset{k_1}{\rightleftharpoons}} 2M_2(L1)(L2) \quad (2)$$

The rate equation for the second-order reversible reaction of **A** + **B** ⇌ 2**C** is given in eq 3, where $[\mathbf{A}] = [\mathbf{A}]_e + \Delta$ and Δ is the displacement from equilibrium:[48]

$$k_1 t = \frac{-\ln\left(\dfrac{\Delta}{\Delta\left(1-\dfrac{4}{K}\right) + [\mathbf{A}]_e + [\mathbf{B}]_e + \left(\dfrac{4}{K}\right)[\mathbf{C}]_e}\right)}{[\mathbf{A}]_e + [\mathbf{B}]_e + \left(\dfrac{4}{K}\right)[\mathbf{C}]_e} \quad (3)$$

The rate equation for a first-order reversible reaction of **A** ⇌ **B** is given as

$$kt = \ln\left(\frac{[\mathbf{A}]_0 - [\mathbf{A}]_e}{[\mathbf{A}]_t - [\mathbf{A}]_e}\right) \quad (4)$$

Ligand exchange reactions between the helicates (**A** + **B** ⇌ 2**C**) were found to be first-order reversible reactions. In the kinetic analyses, the concentrations of **A** and **B** were treated as one compound since baseline separation of the peaks in the ^{1}H NMR spectra was not always possible with the two reactant helicates. The rate constants for the first-order reversible ligand exchange reactions were determined with use of eq 4. Rate constants (k) and half-lives ($t_{1/2}$) for the ligand exchange experiments are given in Table 3. It should be noted that neither intermediates nor free ligands were observed in the ^{1}H NMR spectra for these reactions.

(b) Silver(I) Helicates. Intermolecular ligand exchange between the silver(I) helicates was too fast to be followed by ^{1}H NMR spectroscopy. In both acetone-d_6 and acetonitrile-d_3, equilibrium was achieved within 3−5 min (Table 3, runs 8−11), this being the time required for addition of solvent (dissolution) and acquisition of the first spectrum. Increasing the size of the substituent at C-6 of the pyridyl ring did not slow the rate of ligand exchange in the silver complexes (Table 3, runs 10 and 11 vs runs 8 and 9, respectively). Ligand exchange favors the crossover products in reactions between silver(I) helicates containing bulky isopropyl substituents; for example, an equilibrium ratio of ca. 0.75:1 for **A** plus **B**:**C** (K = 7.5) was found for the (*R**,*R**)-((±))-$[Ag_2(\mathbf{1b})_2](PF_6)_2$−(*R**,*R**)-((±))-$[Ag_2(\mathbf{1c})_2](PF_6)_2$ system in acetone-d_6.

(c) Copper(I) Helicates. Solvent Effect. The rates of ligand exchange for the copper(I) helicates showed a marked solvent effect. For the systems (*R**,*R**)-((±))-$[Cu_2(\mathbf{1a})_2](PF_6)_2$−(*R**,*R**)-((±))-$[Cu_2(\mathbf{1b})_2](PF_6)_2$ and (*R**,*R**)-((±))-$[Cu_2(\mathbf{1b})_2](PF_6)_2$−(*R**,*R**)-((±))-$[Cu_2(\mathbf{1c})_2](PF_6)_2$ at room temperature, equilibrium was reached most rapidly in acetonitrile (Table 3, runs 4 and 6) and least rapidly in acetone (Table 3, runs 1 and 5); acetonitrile is a strongly coordinating ligand for copper(I).

(47) Moriyasu, M.; Hashimoto, Y. *Bull. Chem. Soc. Jpn.* **1980**, *53*, 3590. Moriyasu, M.; Hashimoto, Y. *Bull. Chem. Soc. Jpn.* **1981**, *54*, 3374. Stach, J.; Kirmse, R.; Dietzsch, W.; Lassmann, G.; Belyaeva, V. K.; Marov, I. N. *Inorg. Chim. Acta* **1985**, *96*, 55.

(48) King, E. L. *Int. J. Chem. Kinet.* **1982**, *14*, 1285. See also: Pladziewicz, J. R.; Lesniak, J. S.; Abrahamson, A. J. *J. Chem. Educ.* **1986**, *63*, 850.

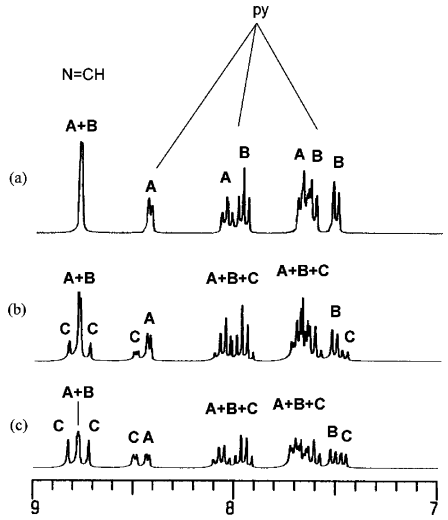

Figure 7. ^{1}H NMR spectra (Me_2CO-d_6, 23 °C, 300 MHz) in azomethine-*H* and py*H* regions for intermolecular ligand exchange reaction between (*R**,*R**)-(±)-[Cu_2(**1a**)$_2$](PF_6)$_2$ (**A**) and (*R**,*R**)-(±)-[Cu_2(**1b**)$_2$](PF_6)$_2$ (**B**) to give crossover helicate (*R**,*R**)-(±)-[Cu_2(**1a**)(**1b**)](PF_6)$_2$ (**C**) at (a) 6 min, (b) 5 days, and (c) 30 days.

The ^{1}H NMR spectra for intermolecular ligand exchange between (*R**,*R**)-((±))-[Cu_2(**1a**)$_2$](PF_6)$_2$ (**A**) and (*R**,*R**)-((±))-[Cu_2(**1b**)$_2$](PF_6)$_2$ (**B**) in acetone-d_6 at 23 °C at 6 min, 5 days, and 30 days are shown in Figure 7. For this system, the two azomethine-*H* resonances for the reactant helicates (**A** and **B**) occur at δ 8.77 and 8.78 ppm. The two singlets overlap significantly—there was no baseline separation of the peaks at either 300 or 500 MHz. The crossover product, (*R**,*R**)-((±))-[Cu_2(**1a**)(**1b**)](PF_6)$_2$ (**C**), contains two azomethine-*H* resonances, one corresponding to coordinated **1a** (δ 8.83), and the other to coordinated **1b** (δ 8.72). There was no baseline separation between the azomethine-*H* resonances for the crossover helicate **C** and the overlapping singlets of the reactant helicates **A** and **B** at 300 MHz, but the separation between the peaks was considered sufficient to allow integration. Thus, the ratio of the reactants (**A** plus **B**) to product (**C**) concentrations was determined.

Determinations of the reactants:product ratios from the azomethine-*H* resonances for this system were also possible by integration of the *H*C-6 pyridine and methyl resonances (Figure 7). The *H*C-6 pyridine resonance in (*R**,*R**)-((±))-[Cu_2(**1a**)$_2$](PF_6)$_2$ occurs as a doublet at δ 8.42 ppm. There are no *H*C-6 pyridine atoms in (*R**,*R**)-((±))-[Cu_2(**1b**)$_2$](PF_6)$_2$, and all other pyridine-*H* resonances occur at lower frequencies (δ 7.5−8.1 ppm). In the crossover product, the corresponding *H*C-6 pyridine resonance occurs at δ 8.49 ppm. Similarly, the methyl resonance occurs at δ 2.14 ppm in the reactant helicate (*R**,*R**)-((±))-[Cu_2(**1b**)$_2$](PF_6)$_2$ and at δ 2.11 ppm in (*R**,*R**)-((±))-[Cu_2(**1a**)(**1b**)](PF_6)$_2$.

The resonances for the crossover helicate (*R**,*R**)-((±))-[Cu_2(**1a**)(**1b**)](PF_6)$_2$ (**C**) were assigned as belonging to either **1a** or **1b** according to the chemical shifts. Peaks such as the methyl and *H*C-6 pyridine resonances were readily assigned, as were some of the nonoverlapping pyridine-*H* resonances. From these few identifiable peaks, it was seen that the resonances corresponding to **1a** in the complex became deshielded when the ligand transferred from the homoleptic complex, (*R**,*R**)-((±))-[Cu_2(**1a**)$_2$](PF_6)$_2$, to the heteroleptic complex, (*R**,*R**)-((±))-[Cu_2(**1a**)(**1b**)](PF_6)$_2$, whereas the resonances corresponding to **1b** experienced more shielding when the ligand transferred from (*R**,*R**)-((±))-[Cu_2(**1b**)$_2$](PF_6)$_2$ to (*R**,*R**)-((±))-[Cu_2(**1a**)(**1b**)](PF_6)$_2$. If this is a general trend, the resonances for the crossover helicate can be assigned according to the relative chemical shifts. Thus, for the azomethine-*H* resonances, the peak at δ 8.83 ppm corresponds to **1a** in **C** (shifted downfield from δ 8.78 in **A**) and the peak at δ 8.72 ppm corresponds to **1b** in **C** (shifted upfield from δ 8.77 in **B**).

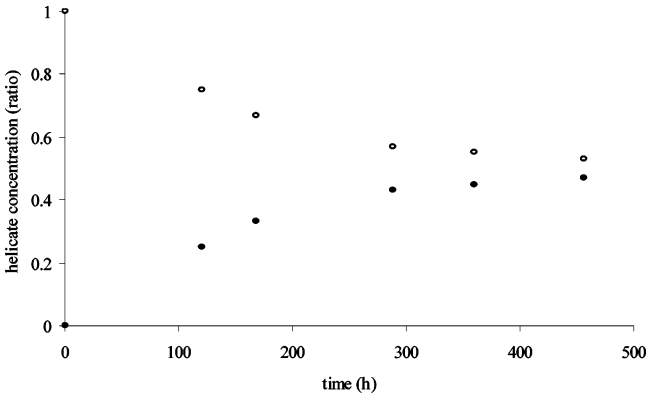

Figure 8. Plot of helicate concentration (ratio) versus time for ligand exchange between (*R**,*R**)-(±)-[Cu_2(**1a**)$_2$](PF_6)$_2$ (**A**) and (*R**,*R**)-(±)-[Cu_2(**1b**)$_2$](PF_6)$_2$ (**B**) to give crossover helicate (*R**,*R**)-(±)-[Cu_2(**1a**)(**1b**)](PF_6)$_2$ (**C**) (Me_2CO-d_6, 23 °C) (○, reactants; ●, product).

A plot of the helicate concentration (ratio) of **A** plus **B** to **C** over time is shown in Figure 8. Application of eq 4 to these data gave a linear plot for the first-order reversible reaction, the slope of the line giving the value for the rate constant, $k = 1.8 \times 10^{-6}$ s^{-1}. The half-life for ligand exchange in this system is 110 h at 23 °C.

Temperature Effect. The effect of temperature on the rate of intermolecular ligand exchange was investigated for the (*R**,*R**)-((±))-[Cu_2(**1a**)$_2$](PF_6)$_2$−(*R**,*R**)-((±))-[Cu_2(**1b**)$_2$](PF_6)$_2$ system in acetone-d_6. A half-life (to equilibrium) of 110 h was obtained for the reaction at 23 °C (Table 3, run 1). The rates of exchange at 45 and 54 °C (Table 3, runs 2 and 3) were also determined by ^{1}H NMR spectroscopy. Again, the ratio of reactants (**A** plus **B**) to product (**C**) helicates was determined by integration of the azomethine-*H* resonances. Spectra obtained on the 500 MHz spectrometer gave baseline separation for the azomethine-*H* peaks of the reactant and product helicates. The equilibrium value achieved was ca. 1:1 for **A** plus **B**:**C** at 45 and 54 °C. The rate constants for the reactions at elevated temperature were 9.3 $\times 10^{-5}$ s^{-1} (45 °C) and 2.1 $\times 10^{-4}$ s^{-1} (54 °C), corresponding to half-lives of 2 and 0.9 h, respectively.

Increasing the temperature of the solution led to an increase in the rate of ligand exchange for the system (Table 3, runs 1−3). The plot of ln k versus $1/T$ for ligand exchange between (*R**,*R**)-((±))-[Cu_2(**1a**)$_2$](PF_6)$_2$ and (*R**,*R**)-((±))-[Cu_2(**1b**)$_2$](PF_6)$_2$ in acetone-d_6 is linear. The Arrhenius activation energy (E_a) for ligand exchange between (*R**,*R**)-((±))-[Cu_2(**1a**)$_2$](PF_6)$_2$ and (*R**,*R**)-((±))-[Cu_2(**1b**)$_2$](PF_6)$_2$ in acetone-d_6 is 130 kJ mol^{-1}, according to these data.

Substituent Effect. The effect of substituent bulk on the rate of ligand exchange between the complexes was investigated. Reactions between (*R**,*R**)-(±)-$[Cu_2(\mathbf{1b})_2](PF_6)_2$ and (*R**,*R**)-(±)-$[Cu_2(\mathbf{1c})_2](PF_6)_2$ in the various solvents allowed a comparison to be made of the effect of substituents at C-6 on the rates of ligand exchange in these double-stranded, dinuclear metal helicates. The rates of ligand exchange between helicates containing bulkier substituents at the C-6 position of the pyridine rings were similar to those with less bulky substituents in this position. The ratio of reactant helicates to product helicate at equilibrium was, however, affected by the substituents.

In acetone-d_6 at 23 °C, the rate of ligand exchange for the system (*R**,*R**)-(±)-$[Cu_2(\mathbf{1b})_2](PF_6)_2$−(*R**,*R**)-(±)-$[Cu_2(\mathbf{1c})_2](PF_6)_2$ was ca. 10^{-6} s^{-1}, a similar value to that obtained for the (*R**,*R**)-(±)-$[Cu_2(\mathbf{1a})_2](PF_6)_2$−(*R**,*R**)-(±)-$[Cu_2(\mathbf{1b})_2](PF_6)_2$ system (see Table 3, run 5 vs run 1). Helicate ratios were determined by integrations of the methyl resonances or by integration of one of the two isopropyl-*Me* resonances in the ^{1}H NMR spectra.

In contrast to the (*R**,*R**)-(±)-$[Cu_2(\mathbf{1a})_2](PF_6)_2$−(*R**,*R**)-(±)-$[Cu_2(\mathbf{1b})_2](PF_6)_2$ system, which reached an equilibrium ratio of ca. 1:1, the (*R**,*R**)-(±)-$[Cu_2(\mathbf{1b})_2](PF_6)_2$−(*R**,*R**)-(±)-$[Cu_2(\mathbf{1c})_2](PF_6)_2$ system favored the product helicate, giving equilibrium ratios of **A** plus **B**:**C** of ca. 45:55. While the rate of exchange did not differ greatly on increasing the steric bulk of the C-6 substituent, the equilibrium was to the right of eq 1 for larger substituents. From these data, it appears that the heteroleptic complex (**C**) is less sterically hindered than the reactant helicate containing two isopropyl-substituted ligands.

(d) Summary of Intermolecular Ligand Exchange between Helicates. Four factors affecting the rates of ligand redistribution between helicates were examined: solvent, substituent, temperature, and metal (Table 3). There was a dramatic difference in the rate of ligand exchange between helicates containing copper(I) and silver(I). Ligand exchange in the silver(I) systems could not be followed by ^{1}H NMR spectroscopy at room temperature because the system had reached equilibrium by the time the first spectrum had been acquired. The effect of solvent on the rate of ligand exchange in the copper(I) helicates was also marked. Reactions in acetonitrile-d_3 were fast compared to the corresponding reactions in acetone-d_6 or dichloromethane-d_2. Increasing the size of the substituent at C-6 of the pyridine ring did not greatly affect the rate of ligand exchange for the copper(I) helicates, although the equilibrium constant was affected by inclusion of the more bulky substituent. The equilibrium constant for the (*R**,*R**)-(±)-$[Cu_2(\mathbf{1a})_2](PF_6)_2$−(*R**,*R**)-(±)-$[Cu_2(\mathbf{1b})_2](PF_6)_2$ system in acetone-d_6 was $K = 4$, whereas the system (*R**,*R**)-(±)-$[Cu_2(\mathbf{1b})_2](PF_6)_2$−(*R**,*R**)-(±)-$[Cu_2(\mathbf{1c})_2](PF_6)_2$ gave $K = 7.5$. An increase in temperature led to an increase in the rate of ligand exchange. The Arrhenius activation energy for the (*R**,*R**)-(±)-$[Cu_2(\mathbf{1a})_2](PF_6)_2$−(*R**,*R**)-(±)-$[Cu_2(\mathbf{1b})_2](PF_6)_2$ system in acetone-d_6 was determined to be 130 kJ mol^{-1}.

These investigations suggest that the double-stranded, dicopper(I) helicates are sufficiently stable for resolution at room temperature, providing that acetonitrile is not used as the solvent.

(2) Intramolecular Inversion. The rates of intramolecular inversion of the dinuclear, double-stranded helicates were investigated with (*R**,*R**)-(±)-$[Cu_2(\mathbf{1c})_2](PF_6)_2$. The two methyls of the isopropyl group in the complexed ligand are diastereotopic and give rise to two doublets in the ^{1}H NMR spectrum. As noted earlier, the backbone CH_2 protons are also diastereotopic in the helicates, but they are accidentally isochronous in the ^{1}H NMR spectra and cannot be used to determine the rates of intramolecular inversion.

Intramolecular inversions not involving bond rupture must occur via transition structures involving metals with square-planar coordination geometries. Thus, for a helicate of the type (*R**,*R**)-(±)-$[Cu_2(\mathbf{1c})_2](PF_6)_2$, the intramolecular inversion (*R*,*R*) ⇌ (*S*,*S*) could occur by either sequential square-planar transition state geometries for the two metal centers or by a concerted mechanism whereby both metal centers are square-planar in the transition state. Inspection of molecular models of the complex indicated that it is unlikely that the copper(I) centers will become planar when the substituents at C-6 are isopropyl groups since their bulk will prevent planar coordination of the diimines around the metal ions. It is more likely that inversion of the metal configuration in the helicate will occur by partial dissociation of the ligands. Support for this contention can be found in the crystal structure of the corresponding silver complex, where a considerable deviation from idealized tetrahedral values is found in the N−Ag−N angles external to the five-membered chelate rings.

To determine the T_c for the coalescence of the isopropyl-*Me* groups in (*R**,*R**)-(±)-$[Cu_2(\mathbf{1c})_2](PF_6)_2$, the complex was dissolved in various solvents and the samples were heated in sealed NMR tubes until coalescence was observed. The rate constants were calculated using $k = \Delta\nu\cdot\pi/\sqrt{2}$, and the free energies were calculated from Eyring's equation, $k = e(-\Delta G^{\ddagger}/RT_c)k_BT_c/h$.

In acetone-d_6, the ^{1}H NMR spectrum of (*R**,*R**)-(±)-$[Cu_2(\mathbf{1c})_2](PF_6)_2$ at 295 K (22 °C) showed the isopropyl-*Me* groups as two doublets ($^3J_{HH}$ = 6.9, 6.9 Hz) with the chemical shift difference $\Delta\delta$ 0.52 ppm. At 382 K, the two doublets ($^3J_{HH}$ = 6.3, 6.6 Hz) were separated by 0.48 ppm. At 391 K, all of the resonances in the ^{1}H NMR spectrum appeared as broad singlets with no coupling observed for any of the proton resonances. The two isopropyl-*Me* peaks appeared as two broad singlets with $\Delta\delta$ 0.48 ppm at this temperature. On cooling of the sample to 295 K, all coupling returned and the spectrum was identical with that obtained before the sample was heated. The rate constant calculated from these data, $k = \Delta\nu\cdot\pi/\sqrt{2} = 350$ s^{-1}, represents the lower limit for intramolecular exchange but is nevertheless much faster than the rate constant for intermolecular ligand exchange between the closely related complexes $[Cu_2(\mathbf{1a})_2](PF_6)_2$ and $[Cu_2(\mathbf{1b})_2](PF_6)_2$ in the same solvent at 23−54 °C, viz. 1.8×10^{-6}−2.1×10^4 s^{-1}. Similar values for the lower limits to the rates of intramolecular exchange for $[Cu_2(\mathbf{1c})_2](PF_6)_2$ were obtained from VT-NMR data in dichloromethane-d_2 and nitromethane-d_3, where there was no

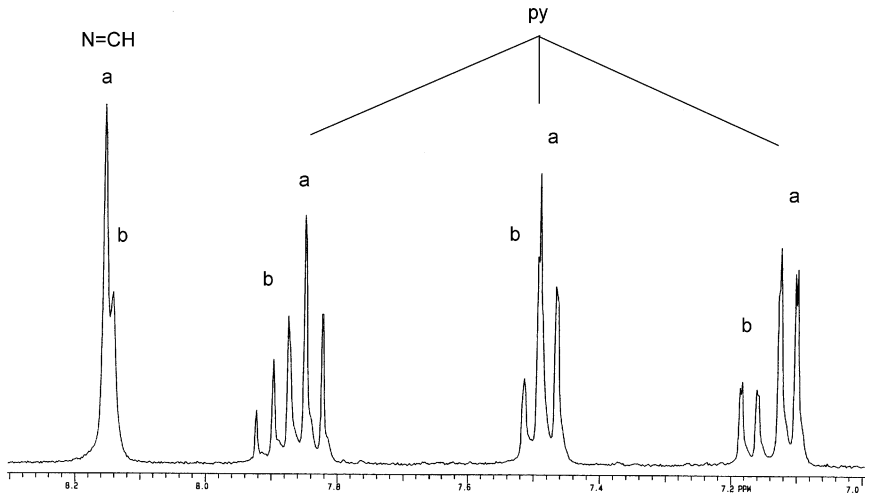

Figure 9. ^{1}H NMR spectrum (CD_2Cl_2, 300 MHz) of a 70:30 mixture of the diastereomers (*R*,*R*)-[Cu_2(**1c**)$_2$]{Δ-(−)-[As(cat)$_3$]}$_2$ and (*S*,*S*)-[Cu_2(**1c**)$_2$]{Δ-(−)-[As(cat)$_3$]}$_2$ (assignments of a and b sets arbitrary) prepared by crystallization of (*R**,*R**)-(±)-[Cu_2(**1c**)$_2$]{Δ-(−)-[As(cat)$_3$]}$_2$ from dichloromethane−diethyl ether−acetone (7:4:1) in the presence of Dabco.

decomposition of the complex. In acetonitrile-d_3, coalescence of the isopropyl-*Me* signals was observed at 380 K, however, but decomposition of the complex was evident in the cooled sample.

Anion Exchange between (*R,*R**)-(±)-[Cu_2(1c)$_2$](PF$_6$)$_2$ and Δ-(−)-K[As(cat)$_3$]. (1) Attempted First-Order Asymmetric Transformation.** Complete anion exchange between (*R**,*R**)-(±)-[Cu_2(**1c**)$_2$](PF$_6$)$_2$ (1 equiv) in dichloromethane-d_2 (which contained a small quantity of Dabco (1,4-diazabicyclo[2.2.2]octane) as proton scavenger) and Δ-(−)-K[As(cat)$_3$][49−52] (2 equiv) in D_2O was confirmed by ^{1}H NMR spectroscopy. The ion-pairing of the arsenate with the helicate was sufficiently strong to distinguish between (*R*,*R*)-[Cu_2(**1c**)$_2$]{Δ-(−)-[As(cat)$_3$]}$_2$ and (*S*,*S*)-[Cu_2(**1c**)$_2$]-{Δ-(−)-[As(cat)$_3$]}$_2$ in solution by ^{1}H NMR spectroscopy. The pyridine-*H* resonances, in particular, showed large diastereomeric splittings, appearing as two sets of overlapping resonances. The isopropyl-C*H*Me$_2$ protons and the methylene protons also showed a doubling-up of their resonances but with significant overlap. The isopropyl-*Me* and azomethine-*H* resonances did not show diastereomeric splittings. Diastereomeric splittings were also not observed in the ^{13}C NMR spectrum of (*R**,*R**)-(±)-[Cu_2(**1c**)$_2$]-{Δ-(−)-[As(cat)$_3$]}$_2$. Despite the strong ion pairing of the diastereomers of the salt in dichloromethane-d_2, there was no significant asymmetric transformation: the ^{1}H NMR spectrum of (*R**,*R**)-(±)-[Cu_2(**1c**)$_2$]{Δ-(−)-[As(cat)$_3$]}$_2$ corresponded to the two diastereomers (*R*,*R*)-[Cu_2(**1c**)$_2$]-{Δ-(−)-[As(cat)$_3$]}$_2$ and (*S*,*S*)-[Cu_2(**1c**)$_2$]{Δ-(−)-[As(cat)$_3$]}$_2$ in almost equal proportions and remained unchanged after 7 days.

Second-Order Asymmetric Transformation.[53] To a freshly prepared dichloromethane/Dabco solution of (*R**,*R**)-(±)-[Cu_2(**1c**)$_2$]{Δ-(−)-[As(cat)$_3$]}$_2$ was added diethyl ether and a small quantity of acetone (solvent ratio dichloromethane:diethyl ether:acetone = 7:4:1). The crystalline powder that precipitated (80% yield) was shown by ^{1}H NMR spectroscopy (CD_2Cl_2/Dabco) to contain the two diastereomers in unequal amounts. Integration of the pyridine-*H* resonances at δ 7.11 and 7.17 ppm gave a 70:30 ratio for the two diastereomers present (40% de) (Figure 9). Within 12 h, however, the ratio of the two sets of resonances in the ^{1}H NMR spectrum had changed to 55:45. Recrystallization of the initial 70:30 mixture of diastereomers from dichloromethane−diethyl ether (1:1) resulted in a crystalline solid, the ^{1}H NMR spectrum of which gave, by integration of the pyridine-*H* resonances, a 55:45 ratio of the two diastereomers (10% de). Further recrystallizations of this 55:45 material using solvent mixtures such as dichloromethane−diethyl ether−acetone and dichloromethane−water−diethyl ether did not improve the de.

Rather than attempting to increase the de by recrystallization of the 70:30 product, a higher de was sought from the initial isolation of the compound from the dichloromethane solution. The two-phase metathesis of (*R**,*R**)-(±)-[Cu_2(**1c**)$_2$](PF$_6$)$_2$ with Δ-(−)-K[As(cat)$_3$] in the presence of Dabco was repeated, and the product was precipitated (91% yield) from the organic phase by the addition of diethyl ether and acetone (5:4:1 dichloromethane−diethyl ether−acetone). The ^{1}H NMR spectrum (CD_2Cl_2/Dabco) of the isolated compound indicated a 77:23 ratio of the two diastereomers. With time, however, the ratio of diastereomers in the solution again reverted to 55:45. The product was unsuitable for crystallography.

Crystallization at Elevated Temperature. In another attempt to increase the de of the copper complex, crystallization from dichloromethane−diethyl ether of a freshly

(49) Rosenheim, A.; Plato, W. *Ber. Dtsch. Chem. Ges.* **1925**, *58B*, 2000. Rosenheim, A.; Baruttschisky, I.; Bulgrin, W.; Plato, W.; Ebert, G. *Z. Anorg. Allg. Chem.* **1931**, *200*, 173.
(50) Ryschkewitsch, G. E.; Garrett, J. M. *J. Am. Chem. Soc.* **1968**, *90*, 7234.
(51) Mason, S. F.; Peart, B. J. *J. Chem. Soc., Dalton Trans.* **1973**, 949. Drake, A. F.; Levey, J. R.; Mason, S. F.; Prosperi, T. *Inorg. Chim. Acta* **1982**, *57*, 151.
(52) Kobayashi, A.; Ito, T.; Marumo, F.; Saito, Y. *Acta Crystallogr., Sect. B: Struct. Crystallogr. Cryst. Chem.* **1972**, *B28*, 3446. Borgias, B. A.; Hardin, G. G.; Raymond, K. N. *Inorg. Chem.* **1986**, *25*, 1057.
(53) Turner, E. E.; Harris, M. M. *Q. Rev. Chem. Soc.* **1947**, *1*, 299. Mason, S. F. *Molecular optical activity and the chiral discriminations*; Cambridge University Press: Cambridge, U.K., 1982; pp 208−211. Harris, M. M. *Prog. Stereochem.* **1958**, *2*, 157.

prepared sample was carried out at 30 °C. The resulting solid, when dissolved in CD_2Cl_2/Dabco, gave a solution containing the two diastereomers of (*R**,*R**)-(±)-[Cu_2(**1c**)$_2$]{Δ-(−)-[As(cat)$_3$]}$_2$ in a 60:40 ratio. The microcrystalline product was unsuitable for a single-crystal X-ray structural determination. Recrystallization of this material from dichloromethane−benzene solution (8:5) gave crystals suitable for X-ray crystallography, however. The initially cloudy dichloromethane−benzene solution became clear after a few hours, with separation of an oil. After a few more hours, the oil began to transform into rosettes of fine needles. These rosettes were left in solution for 3 days, during which time they slowly transformed into plates. After a further 5 days, the crystalline plates were isolated by filtration. The ^{1}H NMR spectrum (CD_2Cl_2/Dabco) of the solid indicated that the two diastereomers were present in a 60:40 ratio. Elemental analyses of the product were consistent with the formula [Cu_2(**1c**)$_2$][As(cat)$_3$]$_2$·CH_2Cl_2.

The crystal isolated for single-crystal X-ray structural determination contained diastereomerically pure (*R*,*R*)-[Cu_2(**1c**)$_2$]{Δ-(−)-[As(cat)$_3$]}$_2$·CH_2Cl_2. Crystallographic data and experimental details for the complex are given in Table 1. Selected interatomic bond lengths and angles for the cation (following the numbering scheme shown in Figure 1) are given in Table 2. The cation crystallizes with the C_2 structure with interatomic bond lengths and angles being similar to those found for (*R**,*R**)-(±)-[Cu_2(**1c**)$_2$](PF_6)$_2$. The copper−copper distance in (*R*,*R*)-[Cu_2(**1c**)$_2$]{Δ-(−)-[As(cat)$_3$]}$_2$ is 3.66 Å. The arsenic−oxygen bond lengths in the anions fell within the range 1.83−1.85 Å, with a regular octahedral coordination geometry for the arsenic.[52]

A second crystal examined was found to contain the same diastereomer of the complex, but this did not prove that the bulk sample was diastereomerically and enantiomerically pure. The ^{1}H NMR spectrum of the product showed the presence of two diastereomers in 60:40 ratio. Thus, either the complex had crystallized by second-order asymmetric transformation as the observed diastereomer having the most favorable lattice energy or the complex had spontaneously resolved as a conglomerate of crystals of the two diastereomers and two of the same diastereomer had been selected for crystallography. If the former case had occurred and there existed only one diastereomer in the solid state, then the barrier for helicate racemization/deracemization must be very low. It was hoped that dissolution of the solid at low temperature would slow the helicate inversion and indicate whether there were two diastereomers or only one diastereomer present in the crystallographic sample.

Low-Temperature NMR Spectroscopy. A precooled (−78 °C) solution of dichloromethane-d_2 (0.65 mL) containing a few crystals of Dabco was added to a pre-cooled (−78 °C) NMR tube containing "(*R*,*R*)-[Cu_2(**1c**)$_2$]{Δ-(−)-[As(cat)$_3$]}$_2$" (9.7 mg). The solid did not dissolve completely in the dichloromethane-d_2 at this temperature, even after 1 h. The partly dissolved sample was introduced into the NMR spectrometer, with the probe temperature set to −70 °C. The first spectrum obtained showed the two diastereomers in ca. 9:1 ratio, but the peaks overlapped and could not be accurately integrated. Within 1 h at −70 °C, however, the ratio of the two diastereomers had become 55:45 (based on the integration of the pyridine-*H* peaks at δ 7.01 and 7.07 ppm). When the sample was removed from the spectrometer, it was noted that there was no longer any undissolved solid.

Table 4. Unit Cell Parameters for (*R*,*R*)-[Cu_2(**1c**)$_2$]{Δ-(−)-[As(cat)$_3$]}$_2$·CH_2Cl_2 Determined by X-ray Powder Diffraction (Bulk Sample) and by Single-Crystal X-ray Structure Determination

param	powder pattern (298 K)	single crystal (200 K)
a, Å	12.357(1)	12.3419(2)
b, Å	26.223(3)	25.9815(4)
c, Å	12.544(1)	12.4508(2)
β, deg	111.54(1)	111.3325(7)
V, Å^3	3780.85	3718.94(10)

An X-ray powder pattern of the bulk sample was accordingly obtained to compare the single-crystal data with data for the bulk sample and to determine whether the solid was a single diastereomer of the complex or a conglomerate of the two diastereomers.

X-ray Powder Diffraction. An X-ray powder diffraction pattern of the bulk sample was collected at 25 °C using a Guinier-Hägg camera with monochromated Cu Kα radiation (λ 1.5406 Å) for $\theta = 0-45°$. Silicon (SRM No. 640c, $a =$ 5.431195(9) Å) was added as an internal standard for accurate determination of the unit cell parameters. The unit cell parameters were calculated from the 105 observed lines of the powder pattern using the program Unitcell.[54] The unit cell parameters determined from the powder pattern (bulk sample) and those found from the single-crystal X-ray structural determination are given in Table 4. A listing of the *d*-spacings and their indexing and intensities for the single-crystal and powder pattern data are given in the Supporting Information.

The unit cell parameters for the bulk sample were marginally different from those found for the single-crystal. This was considered to be due to the temperature difference—the powder pattern was obtained at 25 °C and the single-crystal data were collected at −73 °C. The single crystal gave a smaller unit cell volume than the powder pattern because of the temperature difference.

Each line in the powder pattern was indexed for the unit cell of the single crystal. There were no unaccounted lines in the powder pattern. Thus, the powder pattern of the bulk sample showed that only one compound was present in the crystalline sample; accordingly, the compound crystallized from dichloromethane as diastereomerically pure (*R*,*R*)-[Cu_2(**1c**)$_2$]{Δ-(−)-[As(cat)$_3$]}$_2$·CH_2Cl_2 in a typical second-order asymmetric transformation.

Variable-Temperature NMR Spectroscopy. The observation of (*R*,*R*)-[Cu_2(**1c**)$_2$]{Δ-(−)-[As(cat)$_3$]}$_2$ and (*S*,*S*)-[Cu_2(**1c**)$_2$]{Δ-(−)-[As(cat)$_3$]}$_2$ in solution, yet only (*R*,*R*)-[Cu_2(**1c**)$_2$]{Δ-(−)-[As(cat)$_3$]}$_2$ in the solid state, indicates that the cation undergoes facile racemization. The rate of inversion of the helicate as the arsenate salt is much faster than that observed for intermolecular ligand exchange and for in-

(54) Nolang, B. *Unitcell*; Uppsala University: Uppsala, Sweden, 1993.

tramolecular inversion of the helicate as the hexafluorophosphate salt.

Kinetic studies with the helicates (*R**,*R**)-(±)-$[Cu_2L_2](PF_6)_2$ (L = **1a**−**c**) had indicated that, at 25 °C in dichloromethane-d_2, intermolecular ligand exchange occurred with a half-life of 40 h, and the barrier to intramolecular inversion ($\Delta G^{\ddagger}$) was at least 76 kJ mol^{-1}. If the helicate racemizes rapidly, the arsenate anion must have a large effect on the rate of inversion of the helicate to account for the large differences in the rates observed in the earlier kinetic studies with the hexafluorophosphate salt and the rapid racemization of the arsenate salt. The effect of the anion on the rate of intermolecular ligand exchange of the helicates was accordingly examined. A mixture of (*R**,*R**)-(±)-$[Cu_2(\mathbf{1b})_2](PF_6)_2$ (1 equiv) and (*R**,*R**)-(±)-$[Cu_2(\mathbf{1c})_2](PF_6)_2$ (1 equiv) was dissolved in CD_2Cl_2 containing a crystal of Dabco, and the solution was shaken with a suspension of Δ-(−)-K[As(cat)$_3$]·1.5H_2O (4 equiv) in D_2O. The ^{1}H NMR spectrum of the organic phase recorded 10 min after mixing was consistent with the presence of both helicates, viz. (*R**,*R**)-(±)-$[Cu_2(\mathbf{1b})_2]\{\Delta$-(−)-[As(cat)$_3$]$\}_2$ and (*R**,*R**)-(±)-$[Cu_2(\mathbf{1c})_2]\{\Delta$-(−)-[As(cat)$_3$]$\}_2$. Moreover, there were two sets of resonances for each helicate, due to diastereomeric splitting. The ^{1}H NMR spectrum of the solution recorded after 20 h was unchanged. The resonances for the crossover product $[Cu_2(\mathbf{1b})(\mathbf{1c})]^{2+}$ were not observed in the spectrum. Indeed, after 5 days in solution, the mixture of (*R**,*R**)-(±)-$[Cu_2(\mathbf{1b})_2]^{2+}$−(*R**,*R**)-(±)-$[Cu_2(\mathbf{1c})_2]^{2+}$−4{Δ-(−)-[As(cat)$_3$]$^-$} showed no crossover product. The intermolecular ligand exchange observed for the (*R**,*R**)-(±)-$[Cu_2(\mathbf{1b})_2](PF_6)_2$−(*R**,*R**)-(±)-$[Cu_2(\mathbf{1c})_2](PF_6)_2$ system in dichloromethane-d_2, however, showed crossover product after 3 days. It appears that strong ion-pairing in the arsenate salts of the helicates hinders intermolecular ligand exchange in this solvent.

It has been reported that the anion tris(tetrachlorocatecholato)phosphate(V) (TRISPHAT) did not affect the rate of racemization (as determined by coalesence of diastereotopic isopropyl-*Me* groups) of a mononuclear copper(I) complex.[22] The effect of changing the anion from hexafluorophosphate to Δ-(−)-tris(catecholato)arsenate(V) on the rate of intramolecular inversion of $[Cu_2(\mathbf{1c})_2]^{2+}$ was accordingly examined. A solution of (*R*,*R*)-$[Cu_2(\mathbf{1c})_2]\{\Delta$-(−)-[As(cat)$_3$]$\}_2$ (0.02 g) in CD_2Cl_2 (0.6 mL, containing a crystal of Dabco) was heated to determine the coalescence temperature. At 296 K, the ^{1}H NMR spectrum contained sharp resonances for each proton, with the pyridine-*H* resonances occurring at δ 7.12 and 7.18 ppm and integrating for a 54:46 ratio of the two diastereomers (8% de). At 321.5 K, all of the resonances corresponding to the cation appeared as broad peaks with no coupling. The isopropyl-*Me* peaks remained diastereotopic ($\Delta\delta$ 0.41 ppm) at the elevated temperature. The T_c for the hexafluorophosphate salt of the helicate in CD_2Cl_2 could not be obtained, but it was >383 K. On heating of the arsenate salt, however, the isopropyl-*Me* resonances appeared to coalesce at ca. 371 K. There also appeared at this temperature a number of additional resonances in the ^{1}H NMR spectrum which remained when the sample was cooled to 298 K.

Conclusion

The helicate (*R**,*R**)-(±)-$[Cu_2(\mathbf{1c})_2](PF_6)_2$ readily undergoes anion exchange with Δ-(−)-K[As(cat)$_3$] to give the two diastereomers (*R*,*R*)- and (*S*,*S*)-$[Cu_2(\mathbf{1c})_2]\{\Delta$-(−)-[As(cat)$_3$]$\}_2$ in solution. In the presence of Dabco, the compound crystallizes from the equilibrating mixture as the diastereomerically and enantiomerically pure helicate (*R*,*R*)-$[Cu_2(\mathbf{1c})_2]\{\Delta$-(−)-[As(cat)$_3$]$\}_2$ in a typical second-order asymmetric transformation. The presence of the single diastereomer of the complex in the solid state was confirmed by a comparison of the unit cell parameters and *d*-spacings for the single crystal with those obtained from powder pattern measurements on the bulk sample. The mechanism for inversion of the helicate cation appears to be an intramolecular process because intermolecular ligand exchange between differently substituted helicates as the arsenate salts does not occur on the time scale of the racemization process. This second-order asymmetric transformation of a dicopper(I)−tetraimine helicate is the first-reported example of the isolation of a diastereomerically and enantiomerically pure copper(I) helicate containing achiral ligands.

Experimental Section

General Methods. Reactions involving air-sensitive compounds were performed under a positive pressure of nitrogen using Schlenk techniques. Dry, degassed solvents were obtained by distillation over appropriate drying agents. Tetrakis(acetonitrile)copper(I) hexafluorophosphate was prepared according to the literature method.[55] Manganese(IV) oxide "precipitated active for synthesis" was obtained from Merck. (+)-Tris[3-((heptafluoropropyl)hydroxymethylene)camphorato]europium(III) was used as received from Aldrich.

Routine NMR spectra were measured on a Varian Gemini 300 spectrometer operating at 300 MHz (^{1}H) and 75 MHz (^{13}C). Chemical shifts (δ) are reported in ppm relative to the internal TMS for ^{1}H NMR spectra recorded in chloroform-d_1 or relative to the residual solvent peak for solvents other than chloroform-d_1. For ^{13}C NMR spectra, the chemical shifts are reported relative to the solvent peak. Variable-temperature ^{1}H NMR spectra were measured on a Varian VXR 300S (300 MHz) spectrometer or a Varian Inova (500 MHz) spectrometer using a Wilmad pressure-NMR tube (no. 524-PV-8) for high-temperature measurements. Probe temperatures were determined by the chemical shift of methanol or ethylene glycol.

Melting points were determined using a Reichert hot-stage. Optical rotations were obtained on solutions in a 1 dm cell at 23 °C using a Perkin-Elmer 241 polarimeter. Specific rotations were estimated to be within ±0.5 deg cm^2 g^{-1}. Conductance measurements of the complexes were obtained using a Radiometer CDC 344 immersion electrode in solutions of dry, distilled nitromethane.

Elemental chemical analyses and EI mass spectra were performed by staff within the Research School of Chemistry.

2-Isopropyl-6-methylpyridine (2). This compound was prepared by following the literature procedure for the synthesis of 2-*tert*-butyl-6-methylpyridine.[56] A solution of *N*-isopropyl-2-methylpropanamide[57] (55.0 g, 0.43 mol, prepared from isobutyryl chloride), acetanilide (57.5 g, 0.43 mol), and HMPA (150 mL, 0.86 mol) was

(55) Kubas, G. J. *Inorg. Synth.* **1990**, *28*, 68.
(56) Frejd, T.; Pedersen, E. B.; Lawesson, S.-O. *Tetrahedron* **1973**, *29*, 4215.

heated under reflux for 16 h. The reaction mixture was cooled, water (140 mL) added, and the solution extracted with diethyl ether (5 × 160 mL). The organic phases were combined, dried ($MgSO_4$), and filtered, and the solvent was removed under reduced pressure. Distillation of the residue gave the pure product as a clear, colorless liquid, bp 56−59 °C (15 mmHg). Yield: 17.6 g (31%). ^{1}H NMR ($CDCl_3$; δ): 1.29 (d, $^3J_{HH}$ = 7.0 Hz; 6 H, CH*Me*$_2$); 2.52 (s, 3 H, *Me*); 3.03 (sept, $^3J_{HH}$ = 6.9 Hz, 1 H, C*H*Me$_2$); 6.95 (t, $^3J_{HH}$ = 8.3, 8.2 Hz; 2 H, py*H*); 7.48 (t, $^3J_{HH}$ = 7.7 Hz, 1 H, py*H*). ^{13}C NMR ($CDCl_3$; δ): 22.58 (CH*Me*$_2$); 24.42 (*C*H$_3$); 36.33 (*C*HMe$_2$); 116.66, 120.30, 136.41, 157.19, 166.69 (py).

2-Isopropyl-6-methylpyridine *N*-Oxide (3). This compound was prepared by following an adapted literature procedure.[58] A mixture of **2** (25.8 g, 0.19 mol), glacial acetic acid (120 mL), and 30% aqueous hydrogen peroxide (20 mL) was heated to 85 °C for 6 h. A further 20 mL of aqueous hydrogen peroxide was added, and the mixture was heated to 85 °C for 16 h. Once cooled, the volume of the reaction mixture was reduced to ca. 80 mL under reduced pressure. (***Caution****: heating peroxide*.) Water (160 mL) was added to the residue, and the volume was again reduced to 150 mL. A further 80 mL of water was added, and the volume was reduced to 125 mL. (The presence of peroxide was checked using test-strips obtained from Merck.) To the yellow solution was added chloroform (100 mL) and a saturated aqueous solution of potassium carbonate (50 mL). The layers were separated, and the aqueous phase was extracted with chloroform (3 × 100 mL). The organic phases were combined, dried ($MgSO_4$), and filtered, and the solvent was removed under reduced pressure to give the crude product as a bright yellow liquid containing **3** (83%) and **2** (17%), as indicated by ^{1}H NMR spectroscopy. Yield: 27.6 g (22.9 g **3**, 79%). ^{1}H NMR ($CDCl_3$; δ): 1.30 (d, $^3J_{HH}$ = 6.7 Hz, 6 H, CH*Me*$_2$); 2.54 (s, 3 H, *Me*); 3.85 (sept, $^3J_{HH}$ = 6.9 Hz, 1 H, C*H*Me$_2$); 7.14 (s, 3 H, py*H*). ^{13}C NMR ($CDCl_3$; δ): 18.28 (*C*H$_3$); 20.22 (CH*Me*$_2$); 27.57 (*C*HMe$_2$); 119.87, 123.29, 124.52, 148.75, 157.36 (py).

2-(Hydroxymethyl)-6-isopropylpyridine (4). This compound was prepared by an adapted and modified literature procedure.[59] In a two-necked, 100 mL round-bottom flask equipped with condenser (to N_2) and a pressure-compensating dropping funnel was placed neat trifluoroacetic anhydride (21.5 mL, 0.152 mol). The flask was cooled in an ethanol−ice bath, and then crude **3** (22.9 g, 0.151 mol, plus **2**, 4.7 g) was added slowly over 1 h. (***Caution****: exothermic!*) The reaction mixture gradually became darker in color. Once **3** was added, the orange-colored mixture was stirred for 10 min and then slowly brought to room temperature and stirred for 3.5 h. The mixture was then poured into water (70 mL) and adjusted to pH 13 by the addition of solid sodium hydroxide, resulting in the formation of a second phase. This mixture was extracted with chloroform (3 × 100 mL), and then the organic phases were combined, dried ($MgSO_4$), and filtered and the solvent was removed under reduced pressure. Fractional distillation of the residue at reduced pressure using a Claisen-Vigreux flask gave pure **4** as a bright yellow liquid having bp 118−119 °C (15 mmHg), 14.9 g (65%). Anal. Calcd for $C_9H_{13}NO$: C, 71.49; H, 8.67; N, 9.26. Found: C, 71.43; H, 8.38; N, 8.98. ^{1}H NMR ($CDCl_3$; δ): 1.28 (d, $^3J_{HH}$ = 7.0 Hz, 6 H, CH*Me*$_2$); 3.05 (sept, $^3J_{HH}$ = 6.9 Hz, 1 H, C*H*Me$_2$); 4.73 (s, 2 H, C*H*$_2$OH); 7.06 (d, $^3J_{HH}$ = 7.7 Hz, 2 H, py); 7.59 (t, $^3J_{HH}$ = 7.7, 7.7 Hz, 1 H, py). ^{13}C NMR ($CDCl_3$; δ): 22.33 (CH*Me*$_2$); 35.86 (*C*HMe$_2$); 63.64 (*C*H$_2$-OH); 117.60, 118.84, 136.97, 157.83, 165.91 (py).

6-Isopropyl-2-pyridinecarboxaldehyde (5). This compound was prepared by an adapted and modified literature procedure.[60] A solution of **4** (14.9 g, 0.0987 mol) in diethyl ether (100 mL) was vigorously stirred over active manganese(IV) oxide (51.5 g, 0.592 mol, 6 equiv) at room temperature for 18 h. The solid MnO_2 was then removed by filtration and washed with diethyl ether (3 × 50 mL). The filtrate and washings were combined, dried ($MgSO_4$), and filtered, and the solvent was removed under reduced pressure. Fractional distillation of the residue at reduced pressure using a Claisen-Vigreux flask gave a fraction having bp 92 °C (15 mmHg), 9.80 g, which was shown by ^{1}H NMR spectroscopy to contain **5** (86%) and **2** (3%). This mixture was separated by column chromatography using 1:1 petroleum spirits (bp 60−80 °C)−diethyl ether as eluant to give pure **5** with R_f = 0.81 (R_f for **4** and **2** = 0.63 and 0.2). Anal. Calcd for $C_9H_{11}NO$: C, 72.46; H, 7.43; N, 9.39. Found: C, 72.70; H, 7.41; N, 8.97. ^{1}H NMR ($CDCl_3$; δ): 1.36 (d, $^3J_{HH}$ = 7.1 Hz, 6 H, CH*Me*$_2$); 3.18 (sept, $^3J_{HH}$ = 6.9 Hz, 1 H, C*H*Me$_2$); 7.42 (t, $^3J_{HH}$ = 4.5 Hz, 1 H, C4-py); 7.79 (d, $^3J_{HH}$ = 3.9 Hz, 2 H, C3, C5-py); 10.07 (s, 1 H, C*H*O). ^{13}C NMR ($CDCl_3$; δ): 22.42 (CH*Me*$_2$); 36.20 (*C*HMe$_2$); 119.02, 124.99, 137.19, 152.15, 168.05 (py), 194.11 (*C*HO).

***N*,*N*′-Bis(2-pyridylmethylene)ethane-1,2-diamine (1a).** This compound was prepared according to the literature procedure[61] and was obtained as a cream-colored crystalline powder, mp 66−67 °C (lit.[61] mp 67−68 °C). Yield: 49.6 g (70%). ^{1}H NMR ($CDCl_3$; δ): 4.07 (s, 4 H, C*H*$_2$); 7.29 (m, 2 H, py); 7.72 (dt, 2 H, py); 7.98 (d, $^3J_{HH}$ = 8.1 Hz, 2 H, py); 8.43 (s, 2 H, N=C*H*); 8.62 (d, $^3J_{HH}$ = 4.9 Hz, 2 H, py). ^{13}C NMR ($CDCl_3$; δ): 61.16 (*C*H$_2$); 121.19, 124.61, 136.39, 149.22, 154.13, 163.25 (py, N=*C*H). ^{1}H NMR (Me$_2$CO-d_6; δ): 4.01 (s, 4 H, C*H*$_2$); 7.38 (m, 2 H, py); 7.81 (m, 2 H, py); 8.00 (d, $^3J_{HH}$ = 7.7 Hz, 2 H, py); 8.36 (s, 2 H, N=C*H*); 8.58 (d, $^3J_{HH}$ = 5.0 Hz, 2 H, py). ^{13}C NMR (Me$_2$CO-d_6; δ): 61.81 (*C*H$_2$); 121.14, 125.60, 137.21, 150.15, 155.63, 163.99 (py, N=*C*H).

***N*,*N*′-Bis(6-methyl-2-pyridylmethylene)ethane-1,2-diamine (1b).** This compound was prepared as described in the literature[62] and was isolated as colorless needles, mp 79.5 °C (lit.[62] mp 80 °C). Yield: 4.62 g (72%). ^{1}H NMR ($CDCl_3$; δ): 2.58 (s, 6 H, *Me*); 4.04 (s, 4 H, C*H*$_2$); 7.17 (d, $^3J_{HH}$ = 7.7 Hz, 2 H, py); 7.62 (t, $^3J_{HH}$ = 7.7 Hz, 2 H, py); 7.79 (d, $^3J_{HH}$ = 7.8 Hz, 2 H, py); 8.40 (s, 2 H, N=C*H*). ^{13}C NMR ($CDCl_3$; δ): 24.28 (*C*H$_3$); 61.44 (*C*H$_2$); 118.57, 124.47, 136.79, 153.68, 158.10, 163.65 (py, N=*C*H). ^{1}H NMR (Me$_2$CO-d_6; δ): 2.48 (s, 6 H, *Me*); 3.98 (s, 4 H, C*H*$_2$); 7.24 (d, $^3J_{HH}$ = 7.1 Hz, 2 H, py); 7.67 (t, $^3J_{HH}$ = 7.6, 7.7 Hz, 2 H, py); 7.80 (d, $^3J_{HH}$ = 7.7 Hz, 2 H, py); 8.31 (s, 2 H, N=C*H*). ^{13}C NMR (Me$_2$-CO-d_6; δ): 24.19 (*C*H$_3$); 61.93 (*C*H$_2$); 118.23, 124.82, 137.40, 155.01, 158.71, 164.14 (py, N=*C*H).

***N*,*N*′-Bis(6-isopropyl-2-pyridylmethylene)ethane-1,2-diamine (1c).** To a solution of **5** (7.80 g, 0.052 mol) in degassed ethanol (5 mL) was added 1,2-diaminoethane (1.75 mL, 0.026 mol). The resulting solution was heated to reflux for 30 min and then stirred at room temperature for 16 h. The solvent was removed under reduced pressure to give a yellow oil that solidified on scratching. Filtration of the solid and washing with water gave **1c** as cream-colored crystals, mp 75 °C. Yield: 6.25 g (75%). Anal. Calcd for $C_{20}H_{26}N_4$: C, 74.50; H, 8.13; N, 17.37. Found: C, 73.71; H, 7.99; N, 17.00. ^{1}H NMR ($CDCl_3$; δ): 1.30 (d, $^3J_{HH}$ = 6.8 Hz,

(57) LaPlanche, L. A.; Rogers, M. T. *J. Am. Chem. Soc.* **1964**, *86*, 337. Sonntag, N. O. V. *Chem. Rev.* **1953**, *52*, 237.
(58) Boekelheide, V.; Linn, W. J. *J. Am. Chem. Soc.* **1954**, *76*, 1286.
(59) Konno, K.; Hashimoto, K.; Shirahama, H.; Matsumoto, T. *Heterocycles* **1986**, *24*, 2169.
(60) Papadopoulos, E. P.; Jarrar, A.; Issidorides, C. H. *J. Org. Chem.* **1966**, *31*, 615.
(61) Busch, D. H.; Bailar, J. C. *J. Am. Chem. Soc.* **1956**, *78*, 1137.
(62) Goodwin, H. A.; Lions, F. *J. Am. Chem. Soc.* **1960**, *82*, 5013.

12 H, CHMe_2); 3.08 sept, $^3J_{HH}$ = 7.0 Hz, 2 H, C*H*Me_2); 4.03 (s, 4 H, CH_2); 7.19 (d, $^3J_{HH}$ = 7.7 Hz, 2 H, py); 7.64 (t, $^3J_{HH}$ = 7.7 Hz, 2 H, py); 7.82 (d, $^3J_{HH}$ = 7.7 Hz, 2 H, py); 8.42 (s, 2 H, N=C*H*). ^{13}C NMR ($CDCl_3$; δ): 22.59 (CHMe_2); 36.29 (*C*HMe_2); 61.43 (*C*H_2); 118.46, 121.40, 136.78, 153.70, 164.18, 167.02 (py, N=*C*H). ^{1}H NMR (Me_2CO-d_6; δ): 1.25 (d, $^3J_{HH}$ = 7.1 Hz, 12 H, CHMe_2); 3.04 (sept, $^3J_{HH}$ = 6.9 Hz, 2 H, C*H*Me_2); 3.99 (s, 4 H, CH_2); 7.27 (d, $^3J_{HH}$ = 7.7 Hz, 2 H, py); 7.71 (t, $^3J_{HH}$ = 7.6, 7.7 Hz, 2 H, py); 7.82 (d, $^3J_{HH}$ = 6.8 Hz, 2 H, py); 8.35 (s, 2 H, N=C*H*). ^{13}C NMR (Me_2CO-d_6; δ): 22.71 (CHMe_2); 36.66 (*C*HMe_2); 61.97 (*C*H_2); 118.62, 122.57, 137.63, 154.96, 164.40, 167.44 (py, N=*C*H). EI-MS: *m*/*z* 322.1 amu (M^+, 100%).

General Procedure for the Preparation of (*R,*R**)-(±)-[M_2L_2]-(PF_6)$_2$.** To a solution of tetrakis(acetonitrile)copper(I) hexafluorophosphate or silver(I) hexafluorophosphate (5−20 mmol) in dry, degassed acetonitrile (20−100 mL) at room temperature was added 1 equiv of ligand (**1a**, **1b**, or **1c**). The reaction flasks containing the silver(I) complexes were covered with aluminum foil to eliminate light. An immediate color change was observed, the copper(I) reaction mixtures changing from colorless to dark orange-brown and the silver(I) reaction mixtures turning from colorless to yellow. Precipitations of the complexes were effected by the slow addition of diethyl ether. Recrystallizations from acetonitrile−diethyl ether or acetone−diethyl ether, followed by drying (40 °C at 0.5 mmHg for 6 h), afforded orange-red crystals of the copper(I) complexes and yellow-pale yellow crystals of the silver(I) complexes.

[*T*-4-(*R,*R**)]-(±)-Bis{μ-[*N*,*N*′-bis(2-pyridylmethylene)ethane-1,2-diamine]}dicopper(I) Hexafluorophosphate, (*R**,*R**)-(±)-[Cu_2(**1a**)$_2$](PF_6)$_2$.** Dark orange-red crystals formed, mp 256 °C (dec). Yield: 4.77 g (86%). Anal. Calcd for $C_{28}H_{28}Cu_2F_{12}N_8P_2$: C, 37.64; H, 3.16; N, 12.54. Found: C, 37.40; H, 3.12; N, 12.64. ^{1}H NMR (Me_2CO-d_6; δ): 4.04 (br pent, 8 H, CH_2); 7.67 (m, 8 H, py); 8.05 (t d, $^3J_{HH}$ = 7.7, 8.0 Hz, $^4J_{HH}$ = 1.7 Hz, 4 H, py); 8.43 (d, $^3J_{HH}$ = 4.7 Hz, 4 H, py); 8.77 (s, 4 H, N=C*H*). ^{13}C NMR (Me_2CO-d_6; δ): 61.03 (*C*H_2); 127.60, 129.27, 139.40, 149.68, 151.10, 163.96 (py, N=*C*H). ^{1}H NMR (CD_3CN; δ): 4.20 (s, 8 H, CH_2); 7.46 (d, $^3J_{HH}$ = 7.9 Hz, 4 H, py); 7.57 (d d d, $^3J_{HH}$ = 7.6, 7.8, $^4J_{HH}$ = 1.3 Hz, 4 H, py); 7.92 (t d, $^3J_{HH}$ = 7.7, 7.7 Hz, $^4J_{HH}$ = 1.6 Hz, 4 H, py); 8.23 (d, $^3J_{HH}$ = 5.1 Hz, 4 H, py); 8.48 (s, 4 H, N=C*H*). ^{13}C NMR (CD_3CN; δ): 60.83 (*C*H_2); 127.37, 129.15, 139.39, 149.55, 150.90, 163.53 (py, N=*C*H). ^{1}H NMR (CD_3NO_2; δ): 4.38 (m, CH_2), 7.54 (d d, $^3J_{HH}$ = 7.7 Hz, $^4J_{HH}$ = 1.0 Hz, 4 H, py); 7.62 (d d d, $^3J_{HH}$ = 7.7, 6.6, $^4J_{HH}$ = 1.2 Hz, 4 H, py); 7.99 (d d d, $^3J_{HH}$ = 7.8, 7.7 Hz, $^4J_{HH}$ = 1.5 Hz, 4 H, py); 8.34 (d d, $^3J_{HH}$ = 4.9 Hz, $^4J_{HH}$ = 1.3 Hz, 4 H, py); 8.58 (s, 4 H, N=C*H*). ^{13}C NMR (CD_3NO_2; δ): 61.64 (*C*H_2); 127.88, 129.67, 139.82, 150.07, 151.60, 164.07 (py, N=*C*H). ^{1}H NMR (CD_2Cl_2; δ): 4.28 (br m, 8 H, CH_2); 7.45 (d d, $^3J_{HH}$ = 7.7 Hz, $^4J_{HH}$ = 1.0 Hz, 4 H, py); 7.57 (d d d, $^3J_{HH}$ = 7.7, 7.7 Hz, $^4J_{HH}$ = 1.3 Hz, 4 H, py); 7.89 (d d d, $^3J_{HH}$ = 7.8, 7.7 Hz, $^4J_{HH}$ = 1.6 Hz, 4 H, py); 8.24 (d d, $^3J_{HH}$ = 5.0, $^4J_{HH}$ = 0.8 Hz, 4 H, py); 8.51 (s, 4 H, N=C*H*). ^{13}C NMR (CD_2Cl_2; δ): 60.73 (*C*H_2); 127.08, 128.92, 138.70, 149.12, 150.14, 163.24 (py, N=*C*H).

[*T*-4-(*R,*R**)]-(±)-Bis{μ-[*N*,*N*′-bis(6-methyl-2-pyridylmethylene)ethane-1,2-diamine]}dicopper(I) Hexafluorophosphate, (*R**,*R**)-(±)-[Cu_2(**1b**)$_2$](PF_6)$_2$.** Dark red crystals formed, mp 262 °C (dec). Yield: 8.30 g (99%). Anal. Calcd for $C_{32}H_{36}Cu_2F_{12}N_8P_2$: C, 40.47; H, 3.82; N, 11.80. Found: C, 40.48; H, 3.82; N, 12.18. ^{1}H NMR (Me_2CO-d_6; δ): 2.14 (s, 12 H, *Me*); 4.46 (s, 8 H, CH_2); 7.52 (d, $^3J_{HH}$ = 7.7 Hz, 4 H, py); 7.63 (d, $^3J_{HH}$ = 7.7 Hz, 4 H, py); 7.97 (t, $^3J_{HH}$ = 7.7, 7.7 Hz, 4 H, py); 8.78 (s, 4 H, N=C*H*). ^{13}C NMR (Me_2CO-d_6; δ): 24.29 (*Me*); 61.62 (*C*H_2); 125.39, 129.05, 139.57, 150.42, 158.85, 164.18 (py, N=*C*H). ^{1}H NMR (CD_3CN; δ): 2.03 (s, 12 H, *Me*); 4.21 (s, 8 H, CH_2); 7.29 (d, $^3J_{HH}$ = 7.2 Hz, 4 H, py); 7.49 (d, $^3J_{HH}$ = 8.1 Hz, 4 H, py); 7.83 (t, $^3J_{HH}$ = 7.7, 7.7 Hz, 4 H, py); 8.43 (s, 4 H, N=C*H*). ^{13}C NMR (CD_3CN; δ): 24.32 (*Me*); 61.32 (*C*H_2); 125.12, 128.94, 139.37, 150.15, 158.86, 163.73 (py, N=*C*H). ^{1}H NMR (CD_3NO_2; δ): 2.13 (s, 12 H, *Me*); 4.39 (br s, 8 H, CH_2); 7.38 (d, $^3J_{HH}$ = 7.1 Hz, 4 H, py); 7.56 (d, $^3J_{HH}$ = 7.2 Hz, 4 H, py); 7.90 (t, $^3J_{HH}$ = 7.7, 7.7 Hz, 4 H, py); 8.55 (s, 4 H, N=C*H*). ^{13}C NMR (CD_3NO_2; δ): 24.52 (*Me*); 62.07 (*C*H_2); 125.63, 129.41, 139.87, 150.83, 159.59, 164.29 (py, N=*C*H). ^{1}H NMR (CD_2Cl_2; δ): 2.08 (s, 12 H, *Me*); 4.28 (s, 8 H, CH_2); 7.30 (d, $^3J_{HH}$ = 7.1 Hz, 4 H, py); 7.48 (d, $^3J_{HH}$ = 7.8 Hz, 4 H, py); 7.82 (t, $^3J_{HH}$ = 7.8, 7.7 Hz, 4 H, py); 8.44 (s, 4 H, N=C*H*). ^{13}C NMR (CD_2Cl_2; δ): 24.47 (*Me*); 61.07 (*C*H_2); 124.90, 128.68, 138.84, 149.41, 158.30, 163.27 (py, N=*C*H).

[*T*-4-(*R,*R**)]-(±)-Bis{μ-[*N*,*N*′-bis(6-isopropyl-2-pyridylmethylene)ethane-1,2-diamine]}dicopper(I) Hexafluorophosphate, (*R**,*R**)-(±)-[Cu_2(**1c**)$_2$](PF_6)$_2$.** Dark orange-red crystals formed, mp 264 °C (dec). Yield: 3.24 g (89%). Anal. Calcd for $C_{40}H_{52}Cu_2F_{12}N_8P_2$: C, 45.24; H, 4.94; N, 10.55. Found: C, 45.51; H, 4.99; N, 10.64. ^{1}H NMR (Me_2CO-d_6; δ): 0.75 (d, $^3J_{HH}$ = 6.9 Hz, 12 H, CH*Me*Me); 1.27 (d, $^3J_{HH}$ = 7.0 Hz, 12 H, CHMe*Me*); 2.70 (sept, $^3J_{HH}$ = 7.0 Hz, 4 H, C*H*Me_2); 4.45 (s, 8 H, CH_2); 7.55 (d, $^3J_{HH}$ = 6.6 Hz, 4 H, py); 7.76 (d, $^3J_{HH}$ = 8.8 Hz, 4 H, py); 8.08 (t, $^3J_{HH}$ = 7.8, 7.7 Hz, 4 H, py); 8.67 (s, 4 H, N=C*H*). ^{13}C NMR (Me_2CO-d_6; δ): 21.97, 22.69 (CHMe_2); 38.49 (*C*HMe_2); 61.37 (*C*H_2); 125.65, 126.29, 140.33, 150.10, 164.46, 168.03 (py, N=*C*H). ^{1}H NMR (CD_3CN; δ): 0.67 (d, $^3J_{HH}$ = 7.0 Hz, 12 H, CH*Me*Me); 1.19 (d, $^3J_{HH}$ = 6.9 Hz, 12 H, CHMe*Me*); 2.52 (sept, $^3J_{HH}$ = 7.0 Hz, 4 H, C*H*Me_2); 4.18 (s, 8 H, CH_2); 7.32 (d, $^3J_{HH}$ = 7.5 Hz, 4 H, py); 7.60 (d, $^3J_{HH}$ = 8.0 Hz, 4 H, py); 7.93 (t, $^3J_{HH}$ = 7.8, 7.7 Hz, 4 H, py); 8.34 (s, 4 H, N=C*H*). ^{13}C NMR (CD_3CN; δ): 21.85, 22.59 (CHMe_2); 38.41 (*C*HMe_2); 61.06 (*C*H_2); 125.58, 126.01, 140.11, 149.86, 164.01, 168.01 (py, N=*C*H). ^{1}H NMR (CD_3NO_2; δ): 0.77 (d, $^3J_{HH}$ = 7.0 Hz, 12 H, CH*Me*Me); 1.25 (d, $^3J_{HH}$ = 7.0 Hz, 12 H, CHMe*Me*); 2.69 (sept, $^3J_{HH}$ = 6.9 Hz, 4 H, C*H*Me_2); 4.38 (br s, 8 H, CH_2); 7.40 (d, $^3J_{HH}$ = 7.7 Hz, 4 H, py); 7.67 (d, $^3J_{HH}$ = 7.7 Hz, 4 H, py); 8.01 (t, $^3J_{HH}$ = 7.7, 7.8 Hz, 4 H, py); 8.46 (s, 4 H, N=C*H*). ^{13}C NMR (CD_3NO_2; δ): 22.18, 22.86 (CHMe_2); 39.08 (*C*HMe_2); 126.07, 126.49, 140.58, 150.55, 164.57, 168.74 (py, N=*C*H). ^{1}H NMR (CD_2Cl_2; δ): 0.76 (d, $^3J_{HH}$ = 6.9 Hz, 12 H, CH*Me*Me); 1.22 (d, $^3J_{HH}$ = 7.0 Hz, 12 H, CHMe*Me*); 2.54 (sept, $^3J_{HH}$ = 7.0 Hz, 4 H, C*H*Me_2); 4.25 (s, 8 H, CH_2); 7.32 (d, $^3J_{HH}$ = 7.2 Hz, 4 H, py); 7.56 (d, $^3J_{HH}$ = 7.1 Hz, 4 H, py); 7.95 (t, $^3J_{HH}$ = 7.8, 7.8 Hz, 4 H, py); 8.34 (s, 4 H, N=C*H*). ^{13}C NMR (CD_2Cl_2; δ): 21.84, 22.74 (CHMe_2); 38.28 (*C*HMe_2); 60.70 (*C*H_2); 125.25, 125.75, 139.61, 149.12, 163.52, 167.64 (py, N=*C*H).

[*T*-4-(*R,*R**)]-(±)-Bis{μ-[*N*,*N*′-bis(2-pyridylmethylene)ethane-1,2-diamine]}disilver(I) Hexafluorophosphate, (*R**,*R**)-(±)-[Ag_2(**1a**)$_2$](PF_6)$_2$.** Cream-yellow needles formed, mp 219 °C (dec). Yield: 2.46 g (75%). Anal. Calcd for $C_{28}H_{28}Ag_2F_{12}N_8P_2$: C, 34.24; H, 2.87; N, 11.41. Found: C, 34.15; H, 2.77; N, 11.40. ^{1}H NMR (Me_2CO-d_6; δ): 4.38 (s, 8 H, CH_2); 7.59 (d d d, $^3J_{HH}$ = 7.7, 7.9 Hz, $^4J_{HH}$ = 1.5 Hz, 4 H, py); 7.77 (d, $^3J_{HH}$ = 7.7 Hz, 4 H, py); 8.05 (d t, $^3J_{HH}$ = 7.8, 7.8 Hz, $^4J_{HH}$ = 1.8 Hz, 4 H, py); 8.46 (d, $^3J_{HH}$ = 5.2 Hz, 4 H, py); 8.86 (br s, 4 H, N=C*H*). ^{13}C NMR (Me_2CO-d_6; δ): 61.56 (*C*H_2); 129.11, 129.16, 140.22, 149.59, 151.81, 165.02 (py, N=*C*H). ^{1}H NMR (CD_3CN; δ): 4.17 (s, 8 H, CH_2); 7.46 (d d d, $^3J_{HH}$ = 7.7, 7.7, $^4J_{HH}$ = 1.2 Hz, 4 H, py); 7.55 (d d d, $^3J_{HH}$ = 7.7 Hz, 4 H, py); 7.91 (d t, $^3J_{HH}$ = 7.8, 7.8, $^4J_{HH}$ = 1.6 Hz, 4 H, py); 8.27 (d, $^3J_{HH}$ = 3.8 Hz, 4 H, py); 8.58 (s, 4 H, N=C*H*). ^{13}C NMR (CD_3CN; δ): 61.26 (*C*H_2); 128.90, 140.06, 149.37, 151.62, 164.50, 164.59 (py, N=*C*H).

[*T*-4-(*R,*R**)]-(±)-Bis{μ-[*N*,*N*′-bis(6-methyl-2-pyridylmethylene)ethane-1,2-diamine]}disilver(I) Hexafluorophosphate, (*R**,*R**)-(±)-[Ag$_2$(1b)$_2$](PF$_6$)$_2$.** Pale yellow needles formed, mp 207 °C (dec). Yield: 2.00 g (82%). Anal. Calcd for $C_{32}H_{36}Ag_2F_{12}N_8P_2$: C, 37.02; H, 3.49; N, 10.79. Found: C, 37.20; H, 3.63; N, 11.09. ^{1}H NMR (Me$_2$CO-d_6; δ): 2.33 (s, 12 H, *Me*); 4.42 (s, 8 H, C*H*$_2$); 7.52 (d, $^3J_{HH}$ = 7.7 Hz, 4 H, py); 7.63 (d, $^3J_{HH}$ = 7.6 Hz, 4 H, py); 7.94 (t, $^3J_{HH}$ = 7.8, 7.7 Hz, 4 H, py); 8.91 (d, $^3J_{AgH}$ = 8.4 Hz, 4 H, N=C*H*). ^{13}C NMR (Me$_2$CO-d_6; δ): 25.60 (*Me*); 61.96 (*C*H$_2$); 126.57, 128.92, 140.34, 148.87, 159.82, 165.23 (py, N=*C*H). ^{1}H NMR (CD$_3$CN; δ): 2.20 (s, 12 H, *Me*); 4.18 (s, 8 H, C*H*$_2$); 7.38 (t, $^3J_{HH}$ = 8.8, 8.3 Hz, 8 H, py); 7.79 (t, $^3J_{HH}$ = 7.7, 4 H, py); 8.59 (br t, $^3J_{AgH}$ = 8.1 Hz, 4 H, N=C*H*). ^{13}C NMR (CD$_3$CN; δ): 25.57 (*Me*); 61.66 (*C*H$_2$); 126.31, 128.81, 140.17, 148.61, 159.83, 164.79 (py, N=*C*H).

[*T*-4-(*R,*R**)]-(±)-Bis{μ-[*N*,*N*′-bis(6-isopropyl-2-pyridylmethylene)ethane-1,2-diamine]}disilver(I) Hexafluorophosphate, (*R**,*R**)-(±)-[Ag$_2$(1c)$_2$](PF$_6$)$_2$.** A pale off-white crystalline powder formed, mp 218 °C (dec). Yield: 2.94 g (65%). Anal. Calcd for $C_{40}H_{52}Ag_2F_{12}N_8P_2$: C, 41.76; H, 4.56; N, 9.74. Found: C, 41.86; H, 4.69; N, 9.24. ^{1}H NMR (Me$_2$CO-d_6; δ): 0.93 (d, $^3J_{HH}$ = 6.8 Hz, 12 H, CH*Me*Me); 1.30 (d, $^3J_{HH}$ = 6.9 Hz, 12 H, CHMe*Me*); 2.90 (sept, $^3J_{HH}$ = 7.0 Hz, 4 H, C*H*Me$_2$); 4.42 (s, 8 H, C*H*$_2$); 7.54 (d, $^3J_{HH}$ = 8.2 Hz, 4 H, py); 7.68 (d, $^3J_{HH}$ = 8.1 Hz, 4 H, py); 8.03 (t, $^3J_{HH}$ = 7.7, 7.7 Hz, 4 H, py); 8.82 (d, $^3J_{AgH}$ = 8.9 Hz, 4 H, N=C*H*). ^{13}C NMR (Me$_2$CO-d_6; δ): 22.34, 22.62 (CH*Me*$_2$); 39.57 (*C*HMe$_2$); 61.41 (*C*H$_2$); 125.66, 127.38, 141.07, 148.48, 165.88, 168.50 (py, N=*C*H). ^{1}H NMR (CD$_3$CN; δ): 1.08 (br s, 24 H, CH*MeMe*); 2.73 (sept, $^3J_{HH}$ = 7.0 Hz, 4 H, C*H*Me$_2$); 4.19 (s, 8 H, C*H*$_2$); 7.32 (d, $^3J_{HH}$ = 7.5 Hz, 4 H, py); 7.53 (d, $^3J_{HH}$ = 8.1 Hz, 4 H, py); 7.88 (t, $^3J_{HH}$ = 7.7, 7.8 Hz, 4 H, py); 8.52 (t, $^3J_{AgH}$ = 8.6 Hz, 4 H, N=C*H*). ^{13}C NMR (CD$_3$CN; δ): 22.43, 22.56 (CH*Me*$_2$); 39.59 (*C*HMe)$_2$); 61.29 (*C*H$_2$); 125.68, 127.21, 141.07, 148.39, 165.58, 168.64 (py, N=*C*H). ^{1}H NMR (CD$_3$NO$_2$; δ): 0.95 (d, $^3J_{HH}$ = 7.0 Hz, 12 H, CH*Me*Me); 1.30 (d, $^3J_{HH}$ = 7.0 Hz, 12 H, CHMe*Me*); 2.90 (sept, $^3J_{HH}$ = 7.0 Hz, 4 H, C*H*Me$_2$); 4.38 (side of solvent peak, C*H*$_2$); 7.40 (d, $^3J_{HH}$ = 6.7 Hz, 4 H, py); 7.60 (d, $^3J_{HH}$ = 8.3 Hz, 4 H, py); 7.96 (t, $^3J_{HH}$ = 7.8, 7.7 Hz, 4 H, py); 8.63 (d, $^3J_{AgH}$ = 8.8 Hz, 4 H, N=C*H*). ^{13}C NMR (CD$_3$NO$_2$; δ): 22.55, 22.84 (CH*Me*$_2$); 40.16 (*C*HMe$_2$); 61.91 (*C*H$_2$); 126.07, 127.57, 141.35, 148.94, 165.94, 169.23 (py, N=*C*H). ^{1}H NMR (CD$_2$Cl$_2$; δ): 0.94 (d, $^3J_{HH}$ = 7.0 Hz, 12 H, CH*Me*Me); 1.26 (d, $^3J_{HH}$ = 7.0 Hz, 12 H, CHMe*Me*); 2.74 (sept, $^3J_{HH}$ = 7.0 Hz, 4 H, C*H*Me$_2$); 4.24 (s, 8 H, C*H*$_2$); 7.29 (d, $^3J_{HH}$ = 7.7 Hz, 4 H, py); 7.50 (d, $^3J_{HH}$ = 8.1 Hz, 4 H, py); 7.88 (t, $^3J_{HH}$ = 7.8, 7.7 Hz, 4 H, py); 8.52 (s, $^3J_{AgH}$ = 8.6 Hz, 4 H, N=C*H*). ^{13}C NMR (CD$_2$Cl$_2$; δ): 22.45 (CH*Me*$_2$); 39.40 (*C*HMe$_2$); 60.93 (*C*H$_2$); 125.25, 126.80, 140.35, 147.53, 164.89, 168.10 (py, N=*C*H).

(±)-Tris(catecholato)arsenic(V) acid monohydrate, H[As(cat)$_3$]·H$_2$O, was prepared according to the literature procedure[62] using 80% arsenic acid syrup. ^{1}H NMR (Me$_2$CO-d_6; δ): 6.58 (m, 6 H, [As(cat)$_3$]); 6.66 (m, 6 H + 2 H, [As(cat)$_3$] and free catechol); 6.83 (m, 2 H, free catechol). The ratio of peaks at δ 6.83 and 6.58 ppm gave a ca. 1.2:1 ratio of H[As(cat)$_3$] to free catechol. ^{13}C NMR (Me$_2$CO-d_6; δ): 110.99, 119.19, 146.89 ([As(cat)$_3$]); 116.02, 120.58, 145.76 (free catechol). ^{1}H NMR (D$_2$O) (lit.[64]; δ): 6.70, 6.76 (broad overlapping multiplet). ^{13}C NMR (D$_2$O; δ): 111.41, 116.27, 120.70, 121.10, 143.84.

(+)-Cinchoninium Δ-(−)-tris(catecholato)arsenate(V) was isolated according to the literature procedure[49] using crude (±)-tris(catecholato)arsenic acid monohydrate. The (+)-cinchoninium-(−)-tris(catecholato)arsenate diastereomer precipitated in one crop as colorless needles in 86% yield (based on H[As(cat)$_3$]). After being dried under vacuum (0.05 mmHg) for 4 h, the product gave $[\alpha]^{25}_D$ −255.4 (*c* 0.307, acetone) (lit. $[\alpha]_D$ −259 (*c*, 0.304, acetone);[65] −253.5 (*c* 1.0429, acetone)[49]).

Potassium Δ-(−)-Tris(catecholato)arsenate(V) Sesquihydrate, Δ-(−)-K[As(cat)$_3$]·1.5H$_2$O. This compound was prepared from the (+)-cinchoninium-(−)-arsenate salt according to the literature procedure:[49] $[\alpha]_D$ −560.3 (*c* 0.438, acetone), $[M]_D$ −2607 (lit. for (−)-K[As(cat)$_3$]·H$_2$O $[\alpha]_D$ −580.9 (*c* not specified, acetone),[50] −459.9 (c 0.424, acetone)[49]). Anal. Calcd. for $C_{18}H_{15}AsKO_{7.5}$: C, 46.46; H, 3.25. Found: C, 46.27; H, 3.31. Recrystallization of the *hydrate* from acetone−diethyl ether (1:15) gave Δ-(−)-K[As(cat)$_3$]·Me$_2$CO, $[\alpha]_D$ −521.9 (*c* 0.426, acetone). Anal. Calcd for $C_{21}H_{18}AsKO_7$: C, 50.81; H, 3.66. Found: C, 50.30; H, 3.61. ^{1}H NMR (Me$_2$CO-d_6; δ): 6.56−6.64 (m, Ar *H*). ^{13}C NMR (Me$_2$CO-d_6; δ): 111.13, 119.23, 146.96 (Ar *C*).

Anion Exchange of (*R,*R**)-(±)-[Cu$_2$L$_2$](PF$_6$)$_2$ (L = 1b,c) with Potassium Δ-(−)-Tris(catecholato)arsenate(V). General Procedure for NMR Experiments.** To a suspension of the potassium Δ-(−)-tris(catecholato)arsenate(V)·1.5 H$_2$O (4×10^{-5} mol, 2 equiv) in D$_2$O (0.5 mL) was added a solution of (*R**,*R**)-(±)-[Cu$_2$L$_2$](PF$_6$)$_2$ (2×10^{-5} mol, 1 equiv) in CD$_2$Cl$_2$ (0.5 mL) containing Dabco (ca. 5 mg). The two-phase mixture was vigorously shaken for 5 min, and then the organic phase was transferred to a tube for NMR spectroscopy. The product was not isolated.

(*R,*R**)-(±)-[Cu$_2$(1b)$_2$]{Δ-(−)-[As(cat)$_3$]}$_2$.** The diastereomers of this complex were generated in solution as described above and distinguished in the ^{1}H NMR spectrum. ^{1}H NMR (CD$_2$Cl$_2$; δ): 2.00, 2.01 (2 s, 2 × 12 H, *Me*); 4.08 (br m, 2 × 8 H, C*H*$_2$); 6.57 (m, 2 × 12 H, [As(cat)$_3$]); 6.67 (m, 2 × 12 H, [As(cat)$_3$]); 7.17 (2 d, $^3J_{HH}$ = 8.2,8.4 Hz, 2 × 4 H, py); 7.40 (d, $^3J_{HH}$ = 8.0 Hz, 2 × 4 H, py); 7.74, 7.76 (2 t, $^3J_{HH}$ = 7.7,7.7 Hz, 2 × 4 H, py); 8.24 (s, 2 × 4 H, N=C*H*). ^{13}C NMR (CD$_2$Cl$_2$; δ): 24.54 (*Me*); 61.10 (*C*H$_2$); 110.97, 119.24, 146.18 ([As(cat)$_3$]); 125.01, 128.65, 139.04, 149.29, 158.03, 163.11 (py, N=*C*H).

(*R,*R**)-(±)-[Cu$_2$(1c)$_2$]{Δ-(−)-[As(cat)$_3$]}$_2$.** This complex was prepared as above; the two diastereomers were distinguished in the ^{1}H NMR spectrum. ^{1}H NMR (CD$_2$Cl$_2$; δ): 0.75 (d, $^3J_{HH}$ = 7.0 Hz, 2 × 12 H, CH*Me*$_2$); 1.18 (d, $^3J_{HH}$ = 7.0 Hz, 2 × 12 H, CH*Me*$_2$,); 2.45 (m (overlapping septs), 2 × 4 H, C*H*Me$_2$); 4.07 (br m, 2 × 8 H, C*H*$_2$); 6.58 (m, 2 × 12 H, [As(cat)$_3$]); 6.67 (m, 2 × 12 H, [As(cat)$_3$]); 7.14 (d d, $^3J_{HH}$ = 7.9,8.1 Hz, 2 × 4 H, py); 7.48 (d, $^3J_{HH}$ = 7.1 Hz, 4 H, py); 7.49 (d, $^3J_{HH}$ = 7.3 Hz, 4 H, py); 7.87 (2 × t, $^3J_{HH}$ = 7.9 Hz, 2 × 4 H, py); 8.16 (s, 2 × 4 H, N=C*H*). ^{13}C NMR (CD$_2$Cl$_2$; δ): 21.76, 22.92 (2 × CH*Me*$_2$); 38.23 (*C*HMe$_2$); 60.69 (*C*H$_2$); 110.95, 119.19, 146.11 ([As(cat)$_3$]); 125.22, 125.81, 139.78, 148.89, 163.39, 167.36 (py, N=*C*H).

Anion Exchange of (*R,*R**)-(±)-[Cu$_2$(1c)$_2$](PF$_6$)$_2$ with Potassium Δ-(−)-Tris(catecholato)arsenate(V). (a) Attempted First-Order Asymmetric Transformation.** To a suspension of Δ-(−)-K[As(cat)$_3$] (0.0384 g, 7.736×10^{-5} mol) in D$_2$O (0.5 mL) was added a solution of (*R**,*R**)-(±)-[Cu$_2$(1c)$_2$](PF$_6$)$_2$ (0.0206 g, 1.939×10^{-5} mol) in CD$_2$Cl$_2$ (0.5 mL, containing a few crystals of Dabco). The mixture was shaken for 5 min, and the organic phase was transferred to an NMR tube. ^{1}H NMR (CD$_2$Cl$_2$; δ): 0.76 (d, $^3J_{HH}$ = 6.8 Hz, 12 H, diastereomer A, CH*Me*Me); 0.77 (d, $^3J_{HH}$ = 6.9 Hz, 12 H, diastereomer B, CH*Me*Me); 1.18 (d, $^3J_{HH}$ = 7.0 Hz, 2 × 12 H, A + B, CHMe*Me*); 2.46 (m, 2 × 4 H, A + B, C*H*Me$_2$); 4.09 (br m, A + B, 2 × 8 H, C*H*$_2$); 6.58 (m, 24 H, [As(cat)$_3$]);

(63) Weinland, R. F.; Heinzler, J. *Ber. Dtsch. Chem. Ges.* **1919**, *52B*, 1316.
(64) Mason, J.; Mason, S. F. *Tetrahedron* **1967**, *23*, 1919.
(65) Mann, F. G.; Watson, J. *J. Chem. Soc.* **1947**, 505.

6.68 (m, 24 H, [As(cat)$_3$]); 7.11 (d, $^3J_{HH}$ = 6.6 Hz, 4 H, B, py); 7.17 (d, $^3J_{HH}$ = 7.7 Hz, 4 H, A, py); 7.49 (t, $^3J_{HH}$ = 7.0, 6.8 Hz, 2 × 4 H, A + B, py); 7.84 (t, $^3J_{HH}$ = 7.7, 7.8 Hz, 4 H, B, py); 7.89 (t, $^3J_{HH}$ = 7.8, 7.8 Hz, 4 H, A, py); 8.14 (s, 4 H, A, N=C*H*); 8.15 (s, 4 H, B, N=C*H*). ^{13}C NMR (CD_2Cl_2; δ): 21.81, 22.98 (CH*Me*$_2$); 38.32 (*C*HMe$_2$); 60.74 (*C*H$_2$); 111.03, 119.36, 146.08 ([As(cat)$_3$]); 125.27, 125.89, 139.85, 148.94, 163.45, 167.44 (py, N=*C*H). The spectra were unchanged after 6 d. ^{1}H NMR (3:1 CD_3CN/CD_2Cl_2; δ): 0.60 (d, $^3J_{HH}$ = 6.9 Hz, 12 H, CH*Me*Me); 1.09 (d, $^3J_{HH}$ = 7.0 Hz, 12 H, CHMe*Me*); 2.41 (sept, $^3J_{HH}$ = 6.9 Hz, 4 H, C*H*Me$_2$); 4.05 (s, 8 H, C*H*$_2$); 6.53 (m, 12 H, [As(cat)$_3$]); 6.60 (m, 12 H, [As(cat)$_3$]); 7.19 (d, $^3J_{HH}$ = 7.3 Hz, 4 H, py); 7.48 (d, $^3J_{HH}$ = 8.2 Hz, 4 H, py,); 7.83 (t, $^3J_{HH}$ = 7.7, 7.8 Hz, 4 H, py); 8.19 (s, 4 H, N=C*H*). Removal of the solvent and dissolution of the complex in CD_2Cl_2 gave a ^{1}H NMR spectrum that was identical with that obtained initially, showing the two diastereomers.

(b) Second-Order Asymmetric Transformation To Give (*R*,*R*)-[Cu$_2$(1c)$_2$]{Δ-(−)-[As(cat)$_3$]}$_2$·CH$_2$Cl$_2$. To a suspension of Δ-(−)-K[As(cat)$_3$]·Me$_2$CO (0.1385 g, 2.790 × 10^{-4} mol, 2.2 equiv) and Dabco (0.0087 g, 0.6 equiv) in water (4 mL) was added a solution of (*R**,*R**)-(±)-[Cu$_2$(**1c**)$_2$](PF$_6$)$_2$ (0.1346 g, 1.268 × 10^{-4} mol, 1 equiv) and Dabco (0.0087 g, 0.6 equiv) in dichloromethane (5 mL). The mixture was shaken for 5 min, and then the organic phase transferred to a round-bottomed flask, which was placed in an oil bath (30 °C). The slow addition of diethyl ether to the solution over 3 h gave black crystals. The ^{1}H NMR spectrum (CD_2Cl_2) of a sample corresponded to a 60:40 ratio of the two diastereomers of (*R**,*R**)-(±)-[Cu$_2$(**1c**)$_2$]{Δ-(−)-[As(cat)$_3$]}$_2$. The compound was recrystallized from dichloromethane (8 mL) and benzene (5 mL). The initially cloudy solution became clear after a few hours, with formation of an oil. After a few more hours, the oil crystallized into rosettes of fine needles. After 3 d in solution, the rosettes began to transform into orange-red plates. After a further 5 d in solution, the product was isolated by filtration, mp 219 (dec). Anal. Calcd for C$_{76}$H$_{76}$As$_2$Cu$_2$N$_8$O$_{12}$·CH$_2$Cl$_2$: C, 55.87; H, 4.75; N, 6.77. Found: C, 56.27; H, 4.70; N, 6.79. $[\alpha]^{23}_D$ = −287.4, $[\alpha]_{578}^{23}$ = −299.4, and $[\alpha]_{546}^{23}$ = −335.3 (*c* 0.167, CH_2Cl_2, for 0.1 dm cell length). The ^{1}H NMR spectrum (CD_2Cl_2) was similar to that given above but showed the two diastereomers **A** and **B** in a 40:60 ratio. A single-crystal X-ray structural determination was performed on one of these crystals, and the crystal was found to be the diastereomerically and enantiomerically pure helicate (*R*,*R*)-[Cu$_2$(**1c**)$_2$]{Δ-(−)-[As(cat)$_3$]}$_2$·CH$_2$Cl$_2$, with the following unit cell parameters: *a* = 12.34170(10) Å, *b* = 25.9810(3) Å, *c* = 12.4508(2) Å, β = 111.3326(4)°, and *V* = 3718.81 Å^3. A powder pattern of the bulk sample indicated that the compound had crystallized by second-order asymmetric transformation to give diastereomerically pure (*R*,*R*)-[Cu$_2$(**1c**)$_2$]{Δ-(−)-[As(cat)$_3$]}$_2$·CH$_2$Cl$_2$ with the following unit cell parameters: *a* = 12.357(1) Å, *b* = 26.223(3) Å, *c* = 12.544(1) Å, β = 111.54(1)°, and *V* = 3780.85 Å^3. A list of *d*-spacings for the single crystal and powder patterns is given in the Supporting Information. Crystallization of the compound from the separated organic phase was also accomplished by the addition of diethyl ether−acetone.

Intermolecular Ligand Exchange. ^{1}H NMR spectra for the ligand exchange reactions were recorded on Varian Inova 500 MHz or Varian Gemini 300 MHz spectrometers. Equimolar amounts of the two helicates (ca. 0.02 g each) were dissolved in the solvent (0.7 mL). No precautions were taken to exclude air. The runs performed at higher temperatures (45 and 54 °C) were carried out using a pressure NMR tube. The first spectrum was obtained within 5 min of the addition of the solvent. Integration of the resonances for the azomethine-protons, C-6-pyridyl-protons, or the methyl resonances gave the ratios of reactant to crossover helicates. The reactions were consistent with first-order reversible processes.

Intramolecular Inversion. The coalescence temperatures for (*R**,*R**)-(±)-[Cu$_2$(**1c**)$_2$](PF$_6$)$_2$ and (*R**,*R**)-(±)-[Cu$_2$(**1c**)$_2$]{Δ-(−)-[As(cat)$_3$]}$_2$ were determined from the coalescence of the diastereotopic isopropyl-*Me* resonances. Samples of the helicates (0.015−0.02 g) were dissolved in the solvent (0.7 mL) to give ca. 0.02 M solutions. The experiments were carried out using a pressure NMR tube.

Chiral LSR Experiment. The helicate (ca. 0.020 g, 2 × 10^{-5} mol) and (+)-Eu(hfc)$_3$ (2 × 10^{-5} mol, 1 equiv) were dissolved in CD_2Cl_2 (0.5 mL).

Crystal Structures. Crystal data and experimental parameters for the complexes are given in Table 1. The absolute configuration of (*R*,*R*)-[Cu$_2$(**1c**)$_2$]{Δ-(−)-[As(cat)$_3$]}$_2$·CH$_2$Cl$_2$ was established by refinement of the Flack parameter, final value −0.013(9), and knowledge of the absolute configuration of the anion.[52] The software used for the structural solutions of the four complexes was SIR92.[66] Molecular graphics were produced with ORTEP-3.[67]

Supporting Information Available: Additional crystallographic data in CIF format and X-ray powder diffraction, NMR, and kinetic data. This material is available free of charge via the Internet at http://pubs.acs.org.

IC051478C

(66) Altomare, A.; Cascarano, G.; Giacovazzo, C.; Guagliardi, A.; Burla, M. C.; Polidari, G.; Camalli, M. *J. Appl. Crystallogr.* **1994**, *27*, 435.
(67) Farrugia, L. J. *J. Appl. Crystallogr.* **1997**, *30*, 565.
(68) Watkin, D. J.; Prout, C. K.; Carruthers, J. R.; Betteridge, P. W. *CRYSTALS Issue 10*; Chemical Crystallography Laboratory: Oxford, U.K., 1996.
(69) Mackay, S.; Gilmore, C. J.; Edwards, C.; Stewart, N.; Shankland, K. *maXus Computer Program for the Solution and Refinement of Crystal Structures*; Nonius, Delft, The Netherlands, MacScience, Japan, and University of Glasgow, Glasgow, Scotland, 1999.